INTERNATIONAL ATOMIC ENERGY AGENCY
UNITED NATIONS EDUCATIONAL, SCIENTIFIC AND CULTURAL ORGANIZATION
INTERNATIONAL CENTRE FOR THEORETICAL PHYSICS
I.C.T.P., P.O. BOX 586, 34100 TRIESTE, ITALY, CABLE: CENTRATOM TRIESTE

H4.SMR/383 - 06

WORKSHOP ON REMOTE SENSING TECHNIQUES WITH APPLICATIONS TO AGRICULTURE, WATER AND WEATHER RESOURCES

(27 February - 21 March 1989)

ELECTROMAGNETIC SPECTRUM

ENERGY SOURCES FOR REMOTE SENSING

INTERACTION OF RADIATION WITH ATMOSPHERE

INTERACTION OF RADIATION WITH GROUND TARGETS

REMOTE SENSING SENSORS

REMOTE SENSING SATELLITES

KOTA S. RAO
I.I.T.
Centre of Studies in Resources Engineering
Powai
400 076 Bombay
INDIA

CONTENTS

List of Tables

FIGURES

PHYSICAL ASPECTS OF REMOTE SENSING

INTRODUCTION

Remote sensing may be broadly defined as the collection of information about an object without being in physical contact with the object. Air crafts and satellites are the common platforms from which remote sensing observations are made . The term remote sensing is restricted to the methods that employ electromagnetic energy as the means of detecting and measuring target characteristics. Electromagnetic energy includes light, heat and microwaves.

This definition of remote sensing excludes electrical, magnetic and gravity surveys that measure force fields rather than electromagnetic radiation. Magnetic and electric surveys are commonly made from aircraft but are considered airborne geophysical surveys rather than remote sensing.

1.1 Concepts of Remote Sensing

As indicated in the definition for remote sensing the electro magnetic radiation is employed in extracting the information about the targets. The major regions of the electromagnetic spectrum that are being used in remote sensing are Visible-IR, Thermal and microwave. The details of these are discussed in the next section.

Fig.1.1a illustrates the concepts of remote sensing in a broad sense. In the visible-IR region of remote sensing, the Sun is the source of illumination for all the objects. The radiation emanating from the Sun passes through atmosphere to reach the ground. While passing through the atmosphere it gets attenuated and scattered depending on the wavelength and the atmospheric constituents. The radiation successfully transmitted through the atmosphere will reach the ground targets. Depending on the characteristics of the ground, the radiation reaching the ground partly reflects and partly get absorbed in the targets. The extent of reflection is a characteristic of target properties. The reflected radiation again passes through the atmosphere undergoing the same process as explained earlier. The successfully transmitted radiation reaches the sensors mounted on the satellite.

In thermal remote sensing the source of energy is earth itself. The thermal emission from the earth's surface will undergo absorption in the atmosphere before reaching the sensors

on the satellite. The emission from the earth surface depends on thermal characteristics of the object. Also the absorption in the atmosphere is a characteristic of atmospheric constituents and their spectral properties. The concept of thermal remote sensing is illustrated in Fig.1.1b.

In microwave remote sensing two possibilities exist namely passive and active. The principle of passive remote sensing is similar to that of thermal remote sensing as indicated in Fig1.1b. The microwave emission from the earth's objects undergo absorption/emission in the atmosphere. The combined effect is measured by the microwave radiometers mounted on satellites. The microwave emission is a combined function of thermal properties and dielectric properties. In active microwave remote sensing the target is illuminated by the microwaves transmitted from the sensors onboard the satellite itself. The scattered radiation in the backward direction, that reaches the satellite is recorded by the sensors mounted on satellite. The scattering properties of the targets are functions of the target dielectric constant and geometry.

The presence of atmospheric constituents divides the electromagnetic spectrum used for remote sensing purposes, in to two groups namely windows and Absorption bands. The windows are used for land and sea based studies. The absorption bands are used for atmospheric studies.

Thus the basic concepts needed to be understood in the context of remote sensing are (i) Electromagnetic Spectrum, (ii) Energy sources, (iii) Interaction of EM radiation with atmospheric constituents and earth targets, (iv) The concepts of sensors and satellites. Thus the subsequent chapters are devoted for a det..led discussion on these aspects.

1.2 Need for Remote Sensing

The conventional techniques used for the identification, delineation, quantification and monitoring of natural resources is very time consuming and costly. However, through the use of remote sensing techniques (followed by the computer analysis of data) will be very quick and cost effective. Thus the remote sensing technology offers the following major advantages.

(i) The survey can be completed in a very short time

(ii) Repetitive survey is possible

(iii) Provides synoptic view with large area coverage

(iv) The data is useful for multiple applications

(v) The digital data is compatible for computer analysis

(vi) Cost effective

Thus there is a need to adopt remote sensing technology for the study of natural resources.

2. ELECTROMAGNETIC SPECTRUM

In this chapter, the complete Electromagnetic Spectrum, different regions useful for remote sensing, the sources of these radiations and the type of detectors used are discussed. Also the principles behind the three regions of electromagnetic spectrum (mentioned earlier) used in remote sensing are discussed. The merits and demerits of using different regions of electromagnetic spectrum for remote sensing are covered.

Fig.2.1 shows complete range of EM spectrum. The EM spectrum covers, γ-rays (3×10^{-6} m — 3×10^{-5} m), X-rays (3×10^{-5} - 0.01 μm), ultraviolet UV (0.01μm - 0.4 μm), Visible (0.4 - 0.7 μm) Near IR (0.7 -1.5 μm), middleIR and FarIR,(1.5 - 1mm. The wavelength region 3 μm - 14 μm is generally referred to as Thermal region), microwaves (1 mm - 0.8 m) and radiowaves (0.8 m - 3×10^{6} m). Table2.1 gives a detailed account of spectral names, subnames and wavelength ranges.

The origin of γ-rays is atomic nucleus and scientillation counters are used for its detection. The origins of X-rays and UV are the inner electronic transitions, ionoziation and dissociation processes. The visible-Near IR radiation originates from the valance electrons, medium and far IR radiation originates from vibrational oscillations of molecules. The most commonly used detectors in UV to medium and far IR are photometers, optical mechanical scanners and vidicon cameras, photographic emulsion techniques etc. The microwaves originate from the transitions of rotational energy levels of molecules and the detectors used are radiometers, scatterometers, Radars etc. A detailed account of these aspects are given in Table2.2.

In the visible and near IR (0.4-1.5μm) regions the reflection property of the target is used to distinguish different targets. As visible light cannot penetrate through the materials, it gives only the surface properties. However, it is possible to achieve very high spatial resolution. It is also possible to have multiband approach for the analysis of the data.

In thermal region,(0.8-14 μm) the thermal emission from the target is used to distinguish the targets. Due to conduction the whole target medium gets heated and therefore the emission can be considered as a volume phenomena. By comparing the thermal data acquired, at 6 AM and at 2 PM, it is possible to estimate the thermal inertia of the targets which is a characteristic of the target.

In microwave (1mm - 0.8m) region, the microwave emission and scattering properties are made use of to distinguish different targets. As microwaves can penetrate to some extent in to the targets medium it gives the volume information

The merits & demerits, applicability and uses of these three regions for remote sensing purposes are given in Table 2.3

3. ENERGY SOURCES FOR REMOTE SENSING

Remote sensing techniques are based on two approaches namely passive and active. In passive remote sensing, in case of visible and near IR, the source of radiation is the sun, and in thermal the source of radiation is earth itself. In active remote sensing techniques, the satellite itself carries its own source of radiation such as microwave transmitter.

There are several theories to explain the nature of radiation and its interaction with matter. Out of these theories, the most prominent theories are Electromagnetic theory and photon theory. Depending on the context and phenomena, it is possible to explain all the experimental observations based on either electroc magnetic theory or photon theory. For example to understand the emission of radiation from earth, sun and also the absorption of radiation in the atmosphere, the photon theory is more useful. Whereas with the help of electromagnetic theory it is possible to explain the microwave transmission, reflection, scattering by the earth objects etc. Therefore we will consider here the Planck's photon theory and Maxwell's electromagnetic wave theory.

3.1 Planck's Radiation Law

The quantum nature of radiation has been put forward by Planck to understand the blackbody radiation. According to the quantum theory, the radiation consists of packets of energy called "quanta", travel with velocity of light.

These quanta are related with frequency as follows

$$Q = h\nu \qquad - \quad - \quad - \qquad (3.1)$$

where h - constant of proportionality known as Planck's constant ($h = 6.626 \times 10^{-34}$ W S^{2})

Q - Energy of the Photon

ν - frequency

In terms of wavelength, the above equation can be written as

$$\lambda = \frac{hc}{Q} \quad \text{since } c = \nu\lambda$$

Planck's idea of quantizing radiation led him successfully to the mathematical description of the spectral distribution of radiation emitted from a perfect radiator or black body. Planck's black body radiation law can be expressed as

$$W_\lambda = \frac{2\pi hc^2}{\lambda^5 [\exp(ch/\lambda KT^{-2}) - 1]} \qquad - \quad - \qquad (3.2)$$

where W_λ is the spectral radiant emitance in W m^{-2} μm^{-1}

h - Planck's constant = 6.6256×10^{-34} W S^{2}

c - velocity of light = 2.997925×10^{8} m S^{-1}

K - Boltzmann's constant = 1.308054×10^{-23} WSK^{-1}

T - Absolute temperature in degrees (K)

λ - Wavelength in meters.

A more useful form for eq.(3.2) for calculation purposes is

$$W_\lambda = \frac{3.74141 \times 10^{8}}{\lambda^5 [\exp((1.43879 \times 10)/\lambda T) - 1]} \qquad - \quad - \qquad (3.3)$$

where W_λ is in W m^{-2} μm^{-1}, but λ in this case in micrometres.

Planck's law fits all the experimental data and agrees with formulas derived earlier by other investigators in the wavelength domains where the older formulas are valid. For example when the wavelength becomes very large (in microwave region $hc/\lambda kT \ll 1$, it can be shown from eq.(3.2) that

$$W_\lambda = \frac{2\pi ck}{\lambda^4} T \quad \text{W m}^{-2}\text{ m}^{-1}\text{ A} \qquad - \qquad - \qquad (3.4)$$

which is nothing but the so-called Rayleigh-Jeans law derived before Planck's work. The problem with eq.(3.4) is that it predicts a continual and rapid rise in W_λ when the wavelength becomes small. This is impossible physically because it would mean that bodies would radiate unlimited amounts of energy as λ decreases, a situation known as the "untraviolet catastrophe". Planck's work showed that eq.(3.4) is valid only for long wavelengths and thereby avoids this so-called catastrophe.

If we now let the wavelength become small [$hc/\lambda KT \gg 1$] and substitute this condition into eq.(3.2) it can be shown that

$$W_\lambda = \frac{2\pi hc^2}{\lambda^5} e^{-hc/\lambda KT} \quad \text{watt per square metre per Angstrom.}$$

This equation is identical to an expression known as Wien's law, which was derived by semiemperical means before Planck's work.

By adding together the power radiated per unit area per unit wavelength, W_λ for all wavelengths, one obtains the total power radiated per unit area of a black body, W given by

$$W = \frac{2\pi^5 K^4}{15 c^2 h^3} T^4 \text{ Watts per square metre} \quad - \quad (3.5)$$

Equation (3.5) states that, the total power per unit area of a black body is proportional to the fourth power of the absolute temperature. This is called Stefan-Boltzmann law and is another example of Planck's agreement with earlier work.
that is ,

$$W = \sigma T^4 \text{ watts per square metre} \quad - \quad - \quad (3.6)$$

where σ - is the Stefan-Boltzmann constant; 5.67×10^{-8} W.m^{-2} K^{-4}

Similarly by differentiating the Planck's radiation law one can show that

$$\lambda_{max} \propto \frac{1}{T} \; ; \; \lambda_{max} = a/T \quad - \quad - \quad (3.7)$$

where a = 2898 μm K

The above equation is known as Wein's displacement law which states that the wavelength at which maximum emission occurs is inversely proportional to the physical temperature of the black body.

In case of gray bodies (whose radiation emission power is less than the black bodies) the radiative power is obtained by multiplying with the emissivity term ϵ . Thus

$$W_{\text{nonblack body}} = \epsilon W_{\text{blackbody}} = \epsilon \frac{2\pi^5 K^4}{15 c^2 h^3} T^4 \text{ W.m}^{-2} \quad (3.8)$$

Using the Planck's radiation formula, the radiation spectrum of black bodies of different temperatures are calculated and shown in Fig.3.1. It can be seen from the Fig.3.1 that when temperature is equivalent to 6000 K (approximate temp. of Sun)the maximum emission falls in the visible region. Similarly when the temperature is 300 K (earth's equivalent blackbody temperature) the maximum emission falls in thermal region.

3.2 Electromagnetic theory

In the region of microwave radiation, the electromagnetic wave theory of Maxwell is found to be more appropriate and can explain all the phenomena. Thus in this section the basis for electromagnetic theory of Maxwell has been discussed.

3.2.1 Fundamental Laws of Electricity and Magnetism

The experimental and theoretical research of Coulomb, Ampere, Faraday and others during the last part of the 18th century and the 1st part of the 19th century laid the foundation for an understanding of basic principles of electric and magnetic phenomena.

Coulomb's Law : This law states that the force of attraction or repulsion between two charges is given by :

$$\vec{F} = \frac{q_1 q_2}{4\pi\epsilon r^2} \quad - \quad - \quad - \quad (3.9)$$

where r is the distance between the two charges q_1 and q_2 in a medium characterised by permittivity ϵ . The electric field intensity is defined as the force per unit charge i.e.

$$\vec{E} = \frac{q_1}{4\pi\epsilon r^2} \quad - \quad - \quad (3.10)$$

Faraday's Law : This law states that the electromotive force (emf) induced in a closed path, such as shown in Fig.3.2, is equal to the rate of change of magnetic flux enclosing the path. The path over which the electric intensity is integrated may be in a conductor or in a dielectric medium or in free space. The integral form of Faraday's law is given by equation (3.11) as follows :

$$\oint_C \bar{E} \cdot d\bar{s} = -\frac{d\phi}{dt} \qquad - - - \quad (3.11)$$

where $\phi = \int_S \bar{B} \cdot d\bar{a}$

Here $\bar{E}$ = intensity of electric field

$\bar{B}$ = magnetic flux density

ϕ = magnetic flux

Ampere's Circuital Law: This law states that the line integral of magnetic intensity around a closed path is equal to the current density enclosing the path. This law is illustrated in Fig.(3.3). The integral form of the Ampere's circuital law is as follows :

$$\oint_C \bar{H} \cdot d\bar{s} = i \qquad - \quad - \quad - \quad (3.12)$$

where $i = \int_S \bar{J} \cdot d\bar{a}$

Here $\bar{H}$ = intensity of magnetic field

i = current flowing through the conductor

$\bar{J}$ = current density

The line integral of $\bar{H}.d\bar{s}$ is known as magnetomotive force.

Gauss's Law : Gauss's law for electric field states that the net outward electric flux through any closed surface is equal to the charge enclosed by the surface. In an electrostatic field the electric flux lines begin from positive charges and end on negative charges. However, in time varying fields the electric flux lines can exist as closed loops. Fig.(3.4) illustrates Gauss's law for the electric field. This law can be mathematically represented as follows :

$$\oint_S \bar{D} \cdot d\bar{a} = Q \qquad - \quad - \quad (3.13)$$

where $Q = \int_V \rho \, dv$

Here $\bar{D}$ = electric flux density

Q = total charge

ρ = charge density

Gauss's law for the magnetic field states that the net outward magnetic flux through any closed surface is zero. This can be represented mathematically as follows :

$$\oint_S \bar{B} \cdot d\bar{a} = 0 \qquad - \quad - \quad - \quad (3.14)$$

This is equivalent to stating that the number of magnetic flux lines entering any region is equal to the number of flux lines leaving the region. This shows that there are no isolated magnetic poles or magnetic charges on which the lines of magnetic flux can terminate.

3.2.2 Maxwell's Equations

Maxwell, in a series of brilliant mathematical contributions, skillfully welded the fundamental laws of electromagnetic field concepts into a unified pattern. His introduction of the displacement current and the assumption that this produces a magnetic field led him to the prediction of electromagnetic wave phenomenon. Since his theoretical velocity of propogation of electromagnetic wave proved to be very nearly equal to the velocity of light, Maxwell concluded that light itself is an electromagnetic wave phenomenon.

Maxwell's modification to Ampere's circuital law : Maxwell showed that current 'i' in equation (3.12) must include not only the conduction (or convection) current but also the displacement current. This is necessary in order to explain the electromagnetic wave phenomena in free space or in dielectrics where the conduction (or convection) current may be negligible. The modified Ampere's circuital law can be written as :

$$\oint_C \bar{H}.d\bar{s} = \int_S \left(\frac{\partial \bar{D}}{\partial t} + \bar{J} \right) \cdot d\bar{a} \qquad - \quad - \quad (3.15)$$

where $\partial D / \partial t$ is known as the displacement current density.

Faraday's law, the modified Ampere's law and Gauss's laws for electric and magnetic fields can be expressed in a differential form using divergence and Stokes theorems as follows:

$$\nabla \times \bar{E} = -\frac{\partial \bar{B}}{\partial t} \qquad - \quad - \quad - \quad (3.16)$$

$$\nabla \times \bar{H} = \bar{J} + \frac{\partial \bar{D}}{\partial t} \quad - \quad - \quad - \quad (3.17)$$

$$\nabla \cdot \bar{D} = \rho \quad - \quad - \quad - \quad (3.18)$$

$$\nabla \cdot \bar{B} = 0 \quad - \quad - \quad - \quad (3.19)$$

The above four equations are popularly known as Maxwell's equations. Further it may be noted that

$$\bar{D} = \epsilon \bar{E} \quad - \quad - \quad (3.20)$$

$$\bar{B} = \mu \bar{H} \quad - \quad - \quad (3.21)$$

where ϵ and μ are the permittivity and permeability of the medium respectively.

3.2.3 Wave Equation in Homogeneous Unbounded Media

Through proper mathematical transformation the wave equation for the propogation of electromagnetic field can be derived using the above Maxwell's equations. Here the electromagnetic wave equation for a homogeneous unbounded source free ($J = 0$, $\rho = 0$) media characterised by permeability μ and permittivity ϵ is derived.

Using the curl operations on equation (3.16), it can be shown that

$$\nabla \times (\nabla \times \bar{E}) = - \nabla \times \left(\frac{\partial \bar{B}}{\partial t}\right)$$

Using equation (3.21) the above equation can be written as

$$\nabla \times (\nabla \times \bar{E}) = \frac{-\mu \, \partial (\nabla \times \bar{H})}{\partial t}$$

By substituting the value of $\nabla \times \bar{H}$ from the equation (3.17) the above equation reduces to

$$\nabla \times (\nabla \times \bar{E}) = - \mu \frac{\partial}{\partial t} \left(\frac{\epsilon \, \partial \bar{E}}{\partial t}\right)$$

$$= - \mu \epsilon \frac{\partial^2 \bar{E}}{\partial t^2} \quad - \quad (3.22)$$

From the differential vector analysis it can be shown that

$$\nabla \times (\nabla \times \bar{E}) = \nabla (\nabla \cdot \bar{E}) - \nabla^2 \bar{E}$$

Since the medium is homogeneous and source free, the term $\nabla \cdot \bar{E}$ will vanish. Therefore the above equation reduces to

$$\nabla \times (\nabla \times \bar{E}) = - \nabla^2 \bar{E} \quad - \quad (3.23)$$

Equations (3.22) and (3.23) can be combined giving rise to

$$- \nabla^2 \bar{E} = - \mu \epsilon \frac{\partial^2 \bar{E}}{\partial t^2}$$

or

$$\nabla^2 \bar{E} - \mu \epsilon \frac{\partial^2 \bar{E}}{\partial t^2} = 0 \quad - \quad (3.24)$$

Similarly an equation in terms of magnetic field can also be derived and the final expression is as follows :

$$\nabla^2 \bar{H} - \mu \epsilon \frac{\partial^2 \bar{H}}{\partial t^2} = 0 \quad - \quad - \quad (3.25)$$

The equations (3.24) and (3.25) are known as wave equations for homogeneous media. The propagation of electromagnetic wave is illustrated in figure 3.5

4. INTERACTION WITH ATMOSPHERE

As mentioned earlier, in the contest of remote sensing the electromagnetic radiation has to travel from sun to earth and then back to the satellite. As earth is always covered with atmosphere, the electromagnetic radiation will interact with atmospheric constituents. The type of interactions can be broadly categorized as absorption and scattering. The resonance absorption depends on the atmospheric gases and their characteristic absorption spectra. Fig.4.1 gives an idea about the structure of the atmosphere with height. The principal absorbers of radiation in the atmosphere are water vapour, carbon dioxide, ozone, oxygen and aerosoles.

4.1 Atmospheric absorption

The resonance absorption in the atmosphere takes place whenever the radiation frequency cioncides with the characteristics frequency of the atmospheric constituents. In all other situations the scattering predominates. The characteristic absorption frequencies of the atmosphere are discussed below.

The water vapour absorption bands are located at 0.72 μm, 0.82 μm, 0.93 μm, 1.13 μm, 1.38 μm, 1.86 μm, 2.01 μm, 2.05 μm, 2.68 μm, 3.6 μm, 4.5 μm, 6.3 μm and 17 μm and at microwaves 0.16 cm and 1.5 cm. Water vapour continuum absorption is also important for space remote sensing applications. CO_2 has a number of absorption bands in the Infrared region of the spectrum. The most important band is the broad one centered at about 14.7 μm where the maximum thermal emission of the atmosphere occurs. CO_2 has a series of other bands centered at about 1.4, 1.6, 2.0, 2.7,4.3, 4.8 and 5.2 μms.

Ozone which occurs in a layer extending from 10 to 60 kms in height and is concentrated at about 22 kms, has extremely high absorption in the ultraviolet region. The principle absorption bands of ozone in the UV, Visible and IR are concentrated at about 0.15, 0.25, 0.30, 0.60 and 9.6 μms. Oxygen has absorption in the visible, UV and microwave regions; the visible spectrum is centered between 0.69 and 0.76 μms. The UV absorption spectrum is located in the region between 0.18 and 0.25 μms and the microwave absorption spectrum is centered at about 0.27 cm and 0.5 cms.

4.2 Atmospheric Scattering

The scattering of the radiation by the atmospheric constituents, depends on wavelength, and particle size. The Scattering in the atmosphere is actually a multiple process in which flux scattered by one scattering element can be scattered again by another element. Different types of scattering phenomena are discussed here.

1. Rayleigh Scattering

Rayleigh Scattering is an elastic scattering. This is due to the presence of molecules and very small particles, many times smaller than the wavelength of radiation under consideration.The probability for this scattering is inversely proportional to the fourth power of the wavelength.

2. Mie Scattering

This is due to the presence of particles having diameter approximately equal to the wavelength of the sensing radiation. This is mainly occuring in the lower part of the atmosphere, that is below 4,572 meters. The intensity of Mie scattering is inversely proportional to the wavelength. However, the exponentional ranges from 0.7 to 2. The particles of smoke and dust are responsible for Mie scattering in the visible, near IR and thermal IR regions.

3. Non-selective scattering

This is due to the presence of particles having diameters much larger than the wavelength of the sensing radiation. Examples for these scatters include water droplets and ice fragments in the clouds.

4.3 Atmospheric Windows

In view of absorption and scattering of radiation due to the atmosphere, the electromagnetic spectrum applicable for remote sensing gets divided into two major portions. These are called as atmospheric windows wherein the atmospheric influence is least and absorption regions wherein the atmospheric absorption lines come into picture. Table 4.1 gives windows available for remote sensing of earth resources in the three regions of electgromagnetic spectrum.

In thermal and microwave regions the windows are used for the study of land resources whereas the absorption bands are used for the study of atmosphere.

Fig.4.2 illustrates the spectral irradiance of direct sunlight and after it passes through the earth atmosphere. The stipulated portion gives the atmospheric absorption due to the atmospheric constituents such as O_3, H_2O, Co_2 and O_2

Fig.4.3 illustrates the nadir radiance measured from a satellite in the frequency range 6-26 μms. The windows and absorption bands due to ozone and carbon dioxide are also indicated in the figure. The smooth curves give values of black body radiances at 300 K, 280 K and 260 K. Similarly Fig.4.4 illustrates the transmission of energy through the atmosphere in the wavelength region 1 - 14 μms. Wavelength regions of high transmittance are atmospheric windows. In this wavelength region, the prominent atmospheric constituents, that are responsible for absorption of radiation are O_3, H_2O and CO_2.

Fig.4.5 illustrates influence of atmosphere in the microwave region 1-300 GHz. It may be noted that wherever the resonance absorption takes place the resonance emission also occurs. Therefore in passive microwave remote sensing, the atmospheric emission becomes more important than the atmospheric absorption. As can be seen from the figure, the prominent atmospheric constituents to be considered are H_2O and O_2. H_2O has an emission line at 22.235 GHz, and 183.31GHz , and oxygen has emission lines aroung 60 GHz and 118 GHz. To study the atmospheric watervapour, 22.235 GHz is useful. Similarly to study the vertical temperature profile, the frequencies around 60 GHz are useful. The lower frequencies are useful for the study of land resources.

From the above investigations, the influence of atmosphere on the useful portion of the electromagnetic spectrum can be summarised as follows. The transmission of the atmosphere in the visible is high. The losses there are primarily due to molecular and aerosol scattering, hardly any molecular absorption occurs in a naturally clear, unpolluted atmosphere. As we move out into the near IR (0.7 - 3μm) we encounter several water absorption bands and a CO_2 absorption region at 2.8 μms. In the middle IR (3-8μm) there is a popular window extending from about 3.2 to 4.2 μms. The thermal IR region between 6 and 15 μ ms contains another popular window between 8 and 14 μm, interrupted by an ozone absorption region between 9 and 10 μ ms. There follows beyond 14 μ ms a strong CO_2 absorption region. The spectrum beyond 15 μ m and about 1 mm is not used for remote sensing purposes because of the poor transmission characteristics of the atmosphere (mainly due to water absorption) and also

because of the lack of sensitive detectors and instrumentation for this region. At a wavelength of 1 mm. we are entering the sharp wavelength end of microwave region.

5. INTERACTION OF RADIATION WITH GROUND TARGETS

Interaction of EM radiation with targets is the central theme of remote sensing. The interaction mechanism depends on the nature of the target and the wave band used. For example in the visible and near IR spectrum, the reflection properties of the targets play an important role in discriminating the type of target. Similarly in the thermal portion of EM radiation, thermal inertia and related thermal properties are important for the discrimination of the targets. In the microwave region, the dielectric properties, absorption and scattering properties are the central themes in the discrimination of the targets. All these aspects are briefly touched upon in this chapter.

As can be seen from Fig.5.1 the incident EM wave on a plane surface with definite thickness undergo three types of interactions. The incident wave will be partly reflected into the first medium, partly absorbed in the second medium and the remaining portion will be transmitted in to 3rd medium.

This can be mathematically represented as

$$E_{I(\lambda)} = E_{R(\lambda)} + E_{A(\lambda)} + E_{T(\lambda)} \qquad (5.1)$$

where $E_{I(\lambda)}$ - incident wave energy

$E_{R(\lambda)}$ - reflected wave energy in the first medium

$E_{A(\lambda)}$ - absorbed wave energy in the second medium

$E_{T(\lambda)}$ - transmitted wave energy in to the third medium

Dividing eq.(5.1) by $E_{I(\lambda)}$ we get

$$1 = P_\lambda + \alpha_\lambda + \tau_\lambda \qquad - \qquad (5.2)$$

where P_λ - reflectivity
α_λ - absorptivity
τ_λ - transmittivity

If the second medium is of infinite dimensions, as the case of earth object, the energy that enters into the second medium will be completely absorbed. Thus

$$\tau_\lambda = 0 \qquad - \qquad - \qquad (5.3)$$

Substitute this in (5.2) we get

$$1 = P_\lambda + \alpha_\lambda \qquad - \qquad - \qquad (5.4)$$

i.e $$(\alpha_\lambda) = 1 - P_\lambda \qquad - \qquad - \qquad (5.5)$$

Under thermodynamic equilibrium conditions, the energy that is absorbed will be reemitted again in the form of EM radiation as per the Kirchhoff Law . This is known as the emissivity of the medium and represented as ε_λ

$$\varepsilon_\lambda = \alpha_\lambda \qquad (5.6)$$

Substituting this in equation (5.5), we get

$$\varepsilon_\lambda = 1 - P_{(\lambda)} \qquad (5.7)$$

From the above equation, it is clear that we must understand the reflectivity and emissivity properties of the targets in the context of remote sensing.

5.1 Reflective Properties of the Targets

Using the Maxwell's equations, derived in the earlier sections and with appropriate boundary conditions, the equations for reflection coefficient can be derived as follows :

$$\Gamma_1(\theta,h) = \left| \frac{\mu_2 \cos\theta_1 - \sqrt{\mu_2\varepsilon_2 - \sin^2\theta_1}}{\mu_2 \cos\theta_1 + \sqrt{\mu_2\varepsilon_2 - \sin^2\theta_1}} \right|^2 \qquad - \quad - \quad (5.8)$$

$$\Gamma_1(\theta,v) = \left| \frac{\varepsilon_2 \cos\theta_1 - \sqrt{\mu_2\varepsilon_2 - \sin^2\theta_1}}{\varepsilon_2 \cos\theta_1 + \sqrt{\mu_2\varepsilon_2 - \sin^2\theta_1}} \right|^2 \qquad - \quad - \quad (5.9)$$

where $\Gamma(\theta,h)$ - reflectivity for the Horizontal polarization

$\Gamma(\theta,v)$ - reflectivity for the vertical polarization

μ_2 - permiability of medium

ε_2 - permitivitty of medium.

θ_1 - incident angle

The above equation refers to a particular physical situation where the surface is smooth. This type of reflection is called specular reflection. If the average dimensions of the roughness of surface are of the order of the wavelength of the radiation, diffused reflection (scattering) takes place. This aspect will be discussed in the subsequent chapters. Fig.5.2 represents the reflection coefficient of vegetation, soil, water as a function of wavelength.

5.2. Thermal Properties of the Targets

As per the Planck's theory discussed earlier,any object above 0 K emits radiation at all wavelengths. This has been illustrated in Fig.3.1. It can be seen from this figure that as the temperature of the object increases, the wavelength at which maximum emission will decrease as per Wien's displacement law. Thus for sun, the λ_{max} occurs in the visible portion of the EM spectra and for the earth, the λ_{max} comes in the thermal portion of EM spectra.

As explained earlier, the Planck's radiation formula reduces to the Stefan-radiation formula (eq.3.8). This formula for the gray bodies can be written as

$$W_{\text{gray body}} = \frac{\epsilon\, 2\pi^5 K^3}{15\, c^2 h^3} T^4 \text{ watts m}^{-2}$$

where ϵ - is the emissivity. In thermal region the emissivities of various materials are given in Table 5.1.

This thermal radiation emitted by earth due to its temperature is being used in thermal remote sensing for the discrimination of the objects. Even though all the objects on the earth are exposed to the sunlight equally, different objects acquire temperatures depending on their thermal properties such as thermal conductivity, thermal capacity and thermal inertia. Fig.5.3 shows the diurnal variations of the temperatures of different objects. It can be seen from the above figure that the maximum variation in the temperatures of different objects are observed at 2 PM and at about 6 AM. Thus for a given object, the difference in the temperatures at 2 PM and 6 AM indicates the temperature amplitude of the objects. This temperature amplitude is governed by the thermal properties of the object.

Thus the thermal remote sensing is more fruitful if the data is acquired around 2 PM or around 6 AM. The best approach may be to make use of both the times data collectively for the analysis purpose. As the thermal emission depends on thermal properties of the material, we can consider that the emission can be a volume phenomena. However, it may be noted that only near surface emission can successfully come out of the medium and the emission interior to the body will be absorbed within the object itself.

Heat Transfer

Heat energy is transferred from one place to other by three mechanisms.

- Conduction is the tranafer of heat through a material by molecular interaction. For example the transfer of heat through a pan to cook food.

- Convection is the transfer of heat throughthe physical movement of heated matter. The circulation of heated water and air are examples of convection.

- Radiation transfers heat in the form of electromagnetic waves. Heat from the sun reaches the earth by radiation. In contrast to conduction and convection, which can only transfer heat through matter, radiation can transfer heat through a vacuum.

Thermal Conductivity K

Thermal conductivity K is a measure of the rate at which heat will pass through a material and is expressed as $^{o}C\ Cal.cm^{-1}\ sec^{-1}\ ^{o}C^{-1}$

The number K for a material is the quantity of heat in calories, that will pass through a 1 cm^3 of the material per second when two opposite faces are maintained at 1 ^{o}C difference in temperature.

Thermal Capacity C

Thermal capacity C is the ability of a material to store

heat. It is the number of calories required to raise the temperature of 1 gm of a material by 1 ^{o}C and is expressed in cal. gm^{-1} cm^{-1} $^{o}C^{-1}$.

Thermal Inertia P

Thermal inertia P is a measure of the thermal response of a material to temperature changes and is given in cal. cm^{-1} $sec^{1/2}$ $^{o}C^{-1}$. The thermal inertia may be calculated from the relationship

$$P = (K\rho C)^{1/2} \quad - \quad - \quad (5.10)$$

where K - Thermal conductivity

ρ - density
C - thermal capacity

Table 5.2 lists the thermal properties of geological material and water at 20 ^{o}C. It can be seen from above table that the average thermal conductivity of the material is 0.006 cal cm^{-1} sec^{-1} C^{-1}, which is two orders of magnitude lower than the thermal conductivity of metals. Similarly the thermal capacity of water is greater than any other substances. The thermal inertia increases linearly with increasing density.

5.3 Microwave Emission and Scattering Properties of the Targets

As discussed earlier, in microwave region two types of remote sensing techniques are in use, namely active and passive. In case of passive, the microwave radiation emitted from targets (T_B Brightness temperature) is being detected. The Brightness temperature of the target depends on the temperature and dielectric properties of the targets. The dielectric constant inturn depends on several physical and chemical properties of the targets. In active microwave remote sensing the scattering properties of the targets are considered. These scattering properties mainly depend on dielectric constant and surface geometry. Thus in this section attention is given to discuss emissivity, diclectric constant, surface geometry and scattering.

5.3.1 Brightness Temperature and Emissivity

As per Planck's quantum theory of black body radiation, the object above 0 K emitts electromagnetic energy. The mathematical formula given by Planck (Refer to eq.3.2) is applicable to only black bodies. In case of gray bodies, the physical temperature in the Planck's formula should be replaced with the equivalent brightness temperature, T_B. Also the simplified form of Planck's formula (Rayleigh-Jeans Approximation) can be written as

$$B_{\beta} = \frac{2f^2}{c^2} K T \quad - \quad - \quad (5.11)$$

(for black body)

$$B_{\beta} = \frac{2f^2}{c^2} \cdot K T_{B} \quad - \quad - \quad (5.12)$$

The emissivity 'e' is defined as the ratio of the spectral brightness of the grey body to that of the black body. Thus

$$e = \frac{B_f}{B_f} = \frac{T_B}{T} \quad - \quad - \quad (5.13)$$

or $$T_B = e\,T \quad - \quad (5.14)$$

Thus to understand the brightness temperature it is required to know the emissivity characteristics. Referring to the earlier section, eq.no. 5.7

$$e_{(\gamma)} = 1 - P_{(\gamma)}$$

Also Fresnel reflection equation for reflectivity are given in eq. nos. (5.8) & (5.9)

It can be seen from the Fresnel reflection equation that the dielectric constant of the medium plays an important role in determining the reflectivity. The angular dependence of emissivity for vertical and horizontal polarization are shown in

Fig.5.4.

For Horizontal polarization emissivity decreases with increasing angle whereas for vertical polarization the emissivity increases upto a particular angle and then decreases. This angle is known as Brewster's angle. Fig.5.5 shows the dependence of emissivity, more or less linearly decreases . It may also be noted that the emissivity increases as the frequency increases. As the roughness increases emissivity also increases.

Dielectric constant

Dielectric constant of a substance is one which gives the electric property of body in an electric field. All the substances are made up of molecules or atoms. The negative or positive charge components of the molecules, atoms or ions will be displaced due to the application of an electric field. The term electric moment is used for describing such a system.

Electric moment = e.r

where
e - charge relative to a fixed point
r - radius vector from the fixed to e

The moment of a group of charges whose net charge is zero is called the dipole moment of the system. This dipole moment is the main factor in determining the dielectric constant of a substance.

The term Polarization is the ratio of dipole moment per unit volume.

Polarization = e . r /unit volume

But from Maxwell's Equation the Dielectric constant $\epsilon = D/E$

where D _ Displacement density which is depending on the polarization
E _ electric field intensity

The dielectric constant is a complex quantity which depends on frequency and temperature.

To understand the dielectric constant let us consider a moist soil medium as an example. Fig.5.6 shows the variation of dielectric constant as a function of soil moisture at 1.4 GHz for 3 soil types. It can be seen from the above figure that the dielectric constant increases with moisture content and the rate of increase is high for the sandy soils and relatively low for clay soils. Fig.5.7 shows the dielectric constant dependence on the frequency in the frequency region 1-30 GHz. The real part of dielectric constant decreases as frequency increases and the imaginary part of dielectric constant increases with increase in frequency.

As the dielectric constant increases, the reflectivity or scattering increases. Therefore the emissivity decreases. Table 5.3 gives the dielectric constant of certain materials. Dielectric constant also depends on temperature and salinity.

5.3.2 Back Scattering Coefficient

The systems used in active microwave remote sensing are generally scatterometers, altimeters, side looking airborne radars and synthetic aperture radars. The basic principle of the radar is described by the famous radar equation as follows :

$$P_r = \frac{P_t G^2 \lambda^2 \sigma}{(4\pi)^3 R^4} \qquad (5.15)$$

where P_r = receiving power

P_t = transmitted power

G = Gain of either antenna
λ = wavelength of the transmitted waves
R = Slant Range
σ = Radar differential scattering cross section

The above equation is derived for a target. For an extended area target the above equation can be modified as follows :

$$P_R = \int_{\text{illuminated area}} \frac{P_t \lambda^2 G^2}{(4\pi)^3 R^4} \sigma^o \, dA \qquad (5.16)$$

This above equation refers to the remote sensing situation. The quantity σ^o is called the differential scattering cross-section or cross-section per unit area. Therefore

$$\sigma^{o} = \text{mean value of } \frac{\sigma^{i}}{A_i} \qquad - \quad (5.17)$$

If we consider the differential scattering cross-section per unit projected area rather than per unit ground area, then

$$\sigma^{o} = \text{mean value of } \frac{\sigma^{i}}{A_i \cos} \qquad - \quad (5.18)$$

σ^{o} is also referred to backscattering coefficient. The backscattering coefficient usually depends on the system parameters such as wavelength, polarization, look angle, and the target parameters such as dielectric constant, roughness,slope inhomogenity (vertical and horizontal). The back scattering coefficient decreases with increasing look angle. Similarly the backscattering coefficient increases with increasing soil moisture [Fig.5.8].

Regarding the dependence of backscattering coefficient on surface roughness, first of all it is necessary to define the parameters to characterize the surface roughness. Usually the mean standard height variation σ and the correlation length l are used to represent the rough surface.

The σ and l describe the statistical variation random component of surface height relative to a reference surface.

For one dimensional surface profile, we can calculate σ as follows :

$$\sigma = \left[\frac{1}{N-1} \sum_{i=1}^{N} (Z_i)^2 - N(\bar{Z})^2 \right]^{1/2}$$

where N - no. of samples

Z_i - height of the profile

$$\bar{Z} = \sum_{i=1}^{N} Z_i$$

The surface correlation length l usually defined as the displacement x at which the auto correlation function $\rho(x')$ reduces to 1/e th times of its value

where $\rho_{(x')} = \dfrac{\sum_{i=1}^{N+i-j} Z_i Z_{j+1} - \bar{Z}}{\sum_{i=1}^{N} Z_i^2}$

$\sum_{i=1}^{N} Z_i^2$

Fig.5.9 shows the concepts of scattering of radiation by the rough surfaces. When the surface is smooth all the scattered radiation is in the direction of normal reflection which is known as specular reflection. As the roughness increases the quantity of scattered radiation in all the directions increases. This phenomena is known as diffuse reflection. When the surface is highly random, the scattered power reaches an isotropic distribution which is independent of angle of incidence.

From Fig. 5.10 it can be seen that as the roughness increases, the sensitivity of the backscattering coefficient with reference to look angle decreases. Further it can be observed that the backscattering coefficient is independent of the surface roughness in the look angle 7-10 degrees.

5.3.3 Influence of vegetation on Microwave Remote Sensing

In passive microwave remote sensing the presence of vegetation decreases the sensitivity of brightness temperature to soil moisture. However, influence of vegetation is more in high soil moisture content region. Similarly in active microwave remote sensing the presence of vegetation decreases the sensitivity of backscattering coefficieht to the soil moisture. However, the vegetation effect is predominantly seen in low soil moisture condition (Fig.5.11a,b).

The vegetation effect on backscattering coefficient as per cloud model is as follows.

$$\sigma^{o}_{c}(\theta) = \sigma^{o}_{v}(\theta) + \frac{\sigma^{o}_{s}(\theta)}{L^{2}(\theta)} \quad m^{2} \; m^{-2}$$

where

$\sigma^{o}_{c}(\theta)$ - is canopy or total back scattering coeffient

$\sigma^{o}_{v}(\theta)$ - is the vegetation backscattering coefficient

$\sigma^{o}_{s}(\theta)$ - is the soil backscattering coefficient

$L(\theta)$ - is the one way loss factor of vegetation layer

6. REMOTE SENSING SENSORS

In remote sensing the reflected/emitted/scattered radiation from earth objects will be detected by the sensors mounted onboard the satellite. The utility and application of the data mainly depends on the type of sensor and the resolving power of the sensor.

6.1 Visible-IR sensors

As refered in Table 2.2 for different regions of electromagnetic spectrum different types of detectors/sensors are used to record the radiation. In visible and near IR portion of the electromagnetic spectrum three types of mechanism are in use, namely, Imaging type, Scanning type and push broom type [Linear Image Self Scanning (LISS)] as shown in Fig.6.1.

In Imaging type of Systems, the complete seen information will be snaped at a time and projected by the camera optics on the face plate of a Return Beam Vidieocon. An example of such systems are TV cameras mounted on Bhaskara I & II satellites. RBV camera (Return Beam Vidieocon) mounted onboard in Landsat series of satellites.

The scanning systems use the scanning mirror which projects the image of one resolution element on a single detector. The cross-track scanning covers the imaged swath across the track. In some cases a limited number of detectors are used so that each scan covers a set of cross-track lines instead of a single one. The platform motion carries the imaged swath along the track. Examples of such systems are the Landsat MSS and Thematic Mapper (TM).

The pushbroom images delete the scanning mechanism and use a linear array of detectors to cover all the pixels in the cross-track dimension. This allows a much longer detector dwell time on each surface pixel, thus allowing much higher sensitivity and a narrow band width of observation. Examples of such systems are the SPOT camera and IRS-LISS I & II.

The characteristics of Landsat MSS, Landsat-TM, IRS-LISS, SPOT camera are given in Table 6.1 - 6.4.

6.2 Thermal Infrared Sensors

Thermal Imaging sensors operate in the same fashion as visible and near IR sensors. The major differences are that the signal is usually significantly weaker and presently available detectors are less sensitive. This leads to sensors with lower resolution and longer dwell time, and to the need for cooling the detectors to reduce the thermal noise. The examples of thermal infrared sensors are Heat Capacity Mapping Machine (HCMM) and some of the spectral bands in TM. The characteristics of HCMR are given in Table 6.5.

6.3 Microwave Sensors

As explained earlier in microwave remote sensing there are two types of systems. The passive systems are called Radiometers and the active systems are called Scatterometers, altimeters, Side Looking Airborne Radars and Synthetic Aperture Radars.

6.3.1 Radiometers

In all most all surface applications, imaging microwave radiometers are used instead of nadir line scan system. The imaging is achieved by mechanically scanning the receiving antenna beam across the swath. The satellite motion allows the imaging along the swath (see Fig.6.2). Imaging Radiometers consists of three basic elements namely, (i) an antenna and its associated scanning mechanism which collects incoming radiation from specific beam pointing directions, (ii) a receiver which detects and amplifies the collected radiation within a specified frequency band and (iii) a data handling system which performs digitizing, multiplexing and formatting functions on the received data as well as other calibrations and housekeeping data.

Resolution and Limitation of Radiometer: Two of the most important parameters of radiometers are the ground resolution and measurement accuracy. The specified temperature measurement accuracy of presently available radiometers is 0.1 K The achievable ground resolution of microwave radiometer depends upon the height of the platform and on the beam width of the radiometer antenna. The beam width of a parabolic antenna can be expressed as

$$\phi_B = 1.2 \frac{\lambda}{D} \quad \text{(radians)}$$

where ϕ_B is the antenna beam width

λ - is the wavelength of the receiving radiation, and
D - is the diamneter of the antenna aperture.

From a platform flying at an altitude H, the linear extent of the resolution element will be

$$\Delta\gamma = H.\varphi_B = 1.2\frac{\lambda}{D}.H$$

Now consider the two cases, in which the radiometer the mounted at different atitudes.

(1) Lower altitude :

Let λ = 3 cm
D = 1 m
H = 5 Km (aircraft altitudes)

In this case resolution is 180 m

(2) Higher altitude :

Let λ = 3 cm
D = 1 m
H = 500 Km (satellite altitude).

In this case resolution is 18 Km.

A number of microwave radiometers, have been flown on earth orbiting and planetary missions. For example the Scanning Multichannel Microwave Radiometer (SMMR) was launched on Seasat and Nimbus-7 satellites. The SMMR instrument characteristics are given in Table 6.6.

6.3.2 Scatterometer/Radar

Radar is an acronym for Radio Detection and Ranging. Radar transmits the signals and receives the signal reflected by the target. The return radar signal is given by two sets of parameters namely target and system parameters as explained earlier. The distance of the target from the radar is determined by the time taken by the radar signal to travel to the target and back. The basic principle of the radar is discussed in the earlier sections.

A calibrated radar is known as a Scatterometer. It is used for measuring the backscattering coefficient of the target. There are two ways of calibrating the radar.

- Internal
- External

The internal calibration permits the determination of relative scattering coefficient, whereas the external calibration permits the absolute determination of the scattering coefficient. The internal calibration is done by the ratio method in which a sample of the transmitted signal is passed through the receiver. The external calibration is done with the help of a standard target whose scattered coefficient is known.

6.3.3 Side Looking Airborne Radar (SLAR)

Side Looking airborne radars are normally divided into two groups namely Real aperture radar and Synthetic aperture radar. The real aperture radars depend on the beam width determined by the actual antenna and is known as real aperture SLAR or real aperture radar (RAR). The synthetic aperture radar (SAR) depends upon signal processing to achieve a very narrow beamwidth in the along track direction than that attainable with the real antenna.

In the real aperture system the cylindrical type antenna is mounted along the side of the aircraft which is long in one direction (to achieve narrow azimuth beam) and narrow in the other. The picture taken by SLAR is not snapshot but it is obtained by scanning the terrain. The antenna directs the microwave energy into a narrow fan shaped beam, which defines the narrow path or line across the terrain strip that is approximately normal to the flight track. The antenna is fed with a pulse of microwave energy which propogates at a speed of light within the beam and successively illuminates points along the line. The signal scattered will return to the aircraft. The time delay associated with this received signal gives the distance between the target and the radar.

Resolution of SLAR : The concept of resolution of SLAR is shown in Fig.(6.3). A small resolved area is achieved by transmitting a pulse of short duration τ, with a narrow azimuth beamwidth(β_h). The returned signal received at the antenna at the time t, after transmission, can have a slant range increment from R to $R + \frac{C\tau}{2}$.

The resolution achieved for a rectangular pulse in the slant range direction is $\gamma_R = \frac{C\tau}{2}$

The total time delay experienced by the radar signal going to a point at a slant range R is

$$T = 2R/C$$

But one is usually more interested in the ground range/across the path resolution(also known as range resolution) and can be seen from the resolution geometry (Fig.6.3) of SLAR. That is

$$\gamma_y = \frac{C\tau}{2\sin\theta}$$

γ 2 sin

where θ is the angle of incidence from the vertical. The resolution along track direction (known as azimuthal resolution) is simply the arc length corresponding to the horizontal beamwidth β_h, that is resolution along the track direction is given by

$$\gamma_a = R \cdot \beta_h = \frac{h \beta_h}{\cos \theta}$$

where h is the height of the radar. From the above two equations, it can be noted that across track resolution is degraded at short distances and along track resolution is degraded at long distances. It can also be noted that the across track resolution is independent of the height of the platform of the sensor and the along track resolution is dependent on the height of the platform. Since antenna length is physically limited by aircraft, most real aperture SLARs use wavelength between 3 and 0.8 cm to achieve beamwidth of the order of milliradian, as required for high resolution radar mapping.

6.3.4 Synthetic Aperture Radar (SAR)

The synthetic aperture radar (SAR) system has an advantage over the real aperture radar (RAR) system in that the resolution is independent of the platform altitude. Hence, such a system may be used in either an aircraft or a spacecraft without compromising the resolution. Thus for fine resolution the synthetic aperture radar system calls for a short antenna, whereas the real aperture radar system calls for a very long antenna.

In RAR and SAR systems, the platform moves along a straight path in a direction oblique to (typically at right angles) the target which is to be imaged. The returned signals from the target are filtered out electronically so that the image is reduced from the signal returned from only a narrow path of the beam. In other words, a coherent phase history of the returned signal is generated and further through a signal processing technique, extremely high resolution in azimuth direction is obtained.

The SAR can be considered in different points of view for along track resolution each of which leads to a different implementation. Some of the points of view for synthetic aperture area

- Doppler beam sharpening
- Synthetic aperture approach

The Synthetic aperture and Doppler beam sharpening approach discuss the resolution only in along track direction. The methodology for the across track resolution for SAR is identical to that of SLAR which has been discussed earlier.

Synthetic Aperture Approach : In this approach the attainable along track resolution is substantially finer than the quantity $\lambda R/D$ in the case of RAR. This approach is illustrated in Fig.6.4. As shown in Fig.6.4 the antenna beam has an along track width L

$$L = \beta_h \cdot R$$

The radar antenna on the airborne vehicle is shown at three different locations, A, B and C. At location A, the forward edge of the beam is first intercepting the target; at location B the antenna is abreast of the target and at location C the aft edge of the beam is just leaving the target. Thus, the total possible length of the synthetic aperture L is simply the resolution that would be obtained with the RAR antenna i.e.,

$$L = \beta_h \cdot R$$

Here β_h is the horizontal or along track beamwidth of the real antennna. The target can be seen through a distance L, moved by radar. This means the antenna is synthesised into a length L. Like in passive remote sensing system, an angular resolution for a radar synthesised aperture of length L can be written as follows

$$\beta' = \lambda/L$$

In considering the beamwidth of a synthetic antenna, the affected phase shift associated with a given target due to two way propogation between the antenna and target must also be taken into account. Therefore, effective angular resolution β'' for synthetised aperture antenna length L is

$$\beta'' = \frac{\lambda}{2L}$$

Hence the beamwidth for the synthetic aperture radar is half that for a real aperture having the same length.

Now the linear along track resolution at slant range R becomes

$$\gamma_x = R\,\beta'' = R\,\frac{\lambda}{2L}$$

Substituting the value $L = \beta_h R$, the above equation reduces to

$$\gamma_x = D/2$$

Thus the theoretically achievable along track resolution γ_x is just half the antenna length and is independent of the slant range R and the operating wavelength λ. This implies that the smaller the antenna size D, the better the along track resolution.

7. Remote Sensing Satellites

So far we have discussed about the sources of energy and its interaction with atmospheric gases, target parameters etc. We also discussed the types of sensors required to detect the electromagnetic radiation. These sensors are conveniently placed on the satellites in view of the advantages of satellite remote sensing. Basically there are three categories of satellites namely (i) Geo-synchronous satellites,(ii) Sun-synchronous (polar orbit) and (iii) Low orbit or inclined orbit satellites. Depending on the purpose and the need, these satellites are being used. In this section the orbital parameters of different satellites and their applications are discussed. Table 7.1 gives the orbital parameters of some of the important satellites.

7.1 The Geo-stationary Satellites

The geo-stationary satellite is the one which remains stationary always with respect to a particular geographical location. To satisfy this condition its orbital plane should coincide with the equitorial plane of the earth. Also the period of the satellite should be equivalent to the period of the earth rotationi.e. 24 hours. To satisfy this condition the altitude of the satellite should be of the order of 36000 Kms.

The geostationary satellites are generally used for communication purposes and meteorological applications such as the study of clouds. Some of the Geostationary satellites are INSAT series, METEOSAT, APPLE, GOES, Meteor, ~~TIROS-N~~.

7.2 Sun Synchronous Satellites

The second category of the satellites are the sun synchronous satellites. The meaning of this is that whenever the satellite arrives over a particular geographical location it always arrives at the same local time. To achieve this condition, the period of the satellite should be of the order 1-1/2 hour and the inclination should be close to 90 degrees. In this situation it is possible to cover the complete globe once in every 15 days or so. The altitude of the satellite is around 1000 Kms. However, the actual orbital parameters will depend on the weight of the satellite.

Sun Synchronous satellites are extensively used for earth resources studies because of its repetitive coverage under similar illumination conditions. Some of the examples of these are Landsat series, IRS, SPOT, NIMBUS series, Seasat, NOAA series, Landsat series, ERS-I.

7.3 Low Orbit Satellites

The third category of satellites are low orbit satellites. These satellites will have the altitude arouned 400 Km with an inclination of the orbital plane of about 45 with the equitorial plane. The period of these satellites are less than the sun-synchronous satellites. These satellites are also used for remote sensing purposes. Some of the examples for these types of satellites are Bhaskara I & II, SIR-A & B, MOMS.

TABLE 2.1

Names of Wavelength Regions

Spectrum name	Spectrum subname	Wavelength
Ultraviolet	Far-ultraviolet (FUV)	0.01-0.20 um
	Middle ultraviolet (MUV)	0.20-0.30 um
	Near ultraviolet (NUV)	0.30-0.38 um
Visible	Violet	0.38-0.45 um
	Blue	0.45-0.49 um
	Green	0.49-0.56 um
	Yellow	0.56-0.59 um
	Orange	0.59-0.63 um
	Red	0.63-0.76 um
Infrared	Near infrared (NIR)	0.80-1.50 um
	Short-wavelength infrared (SWIR)	1.50-3.00 um
	Middle-wavelength infrared (MWIR)	3.00-5.00 um
	Long-wavelength infrared (LWIR)	5.00-15.0 um
	Far infrared (FIR)	15.0-300.0 um
Microwave	Submillimeter	0.01-0.10 cm
	Millimeter	0.10-1.00 cm
	Microwave	1.0-100.0 cm

TABLE 2.2

Remote Sensor Types and Applications

Remote Sensors	Comments
Scintillation counters Gamma-ray spectrometer, Geiger counters <0.003 - 10 nm	Measurement of emitted natural radiation by gamma ray detectors: NaI,film,etc.
Scanners with photomultipliers Image orthicons and cameras with filtered infrared film >2900 A 10 - 400 nm	Records incident natural radiation. Imaged ultra-violet spectroscopy available.
Cameras Using conventional B&W and color film 0.4 - 0.7 um	B&W film for high spatial detail. Improved spatial detail through contrast.
Using infrared film (B&W and IR color) 0.6 - 0.9 um	Greater reflectance gradients useful for vegetation surveys.
Multispectral units 0.3 - 0.9 um	Individual narrow band scenes available with multi-camera systems
Lidar Laser radar 0.4 - 1.1 um	Monochromatic active system for measureing backscattered EMR from atmosphere, particularly particulates.
Radiometers (infrared) Thermal IR band 2.5 - 14 um	Generally measures total radiation in a wide band in the infrared region. Imagery obtained by scanning techniques.

TABLE 2.2 continuation

Remote sensor types and applications

Remote sensor	Comments
Photometers 0.4 - 0.7 um	Measures luminous flux in various bands of the optical region for distribution, color, etc.
Spectrometers In any spectral region	Narrow-band data available sequentially-EMR amplitude vs frequency.
Solid-state detectors Single detectors Linear arrays Matrices 1.0 um - 1.0 mm	Single detecting element used in scanners, radiometers. One-and two-dimensional arrays for sequential data gathering.
Radars 1 mm-0.8 m	Narrow-band active systems. Both analog data and imagery available.
Radiometers (microwave) 1 mm - 0.8 m	Passive systems. Both analog and imagery available.

TABLE 2.3

Comparison of different Remote Sensing Approaches

Sensor	Advantage	Disadvantages	Noise source
Visible and infrared (0.3-3 um)	High resolution	Very less penetration power (it responds only to a thin surface layer); cloud cover limits frequency of coverage; the physical concepts are not adequate to analyse the data	Surface roughness, surface cover, atmospheric attenuation
Thermal infrared (10-12 um)	High resolution is possible (400 M) large swath width basic physics well understood Day-night capability	Cloud cover limits frequency of coverage	Local meteorological condition partial vegetation cover, surface topography
Passive microwave (1-50 cm) (0.6-30 GHz)	Independent of atmosphere and cloud cover; moderate vegetation penetration, independent of sun illumination all weather capability and day/night capability	Poor spatial resolution (5-10 KM) interference from man made limits operating wavelengths	Surface roughness vegetative cover temperature
Active microwave (1-50 cm) (0.6-30 GHz)	Independent of atmosphere and cloud cover, high resolution possible, independent of sun illumination all weather and day/night capability	Limited swath width and calibration of SAR	Surface roughness slope, vegetative cover

TABLE 4.1

Major Atmospheric Windows Available for Spacecraft Sensing
(Clearest Windows shown in Boldface)

Ultraviolet and visible	**0.30-0.75 um** **0.77-0.91**
Near-infrared	1.0-1.12 1.19-1.34 **1.55-1.75** **2.05-2.4**
Mid-infrared	3.5-4.16 4.5-5.0
Thermal infrared	8.0-9.2 **10.2-12.4** 17.0-22.0
Microwave	2.06-2.22 mm 3.0-3.75 **7.5-11.5** **20.0+**

TABLES 5.1

Emissivity of representative samples of various materials determined in the 8 to 12 um wavelength region

Material	Emissivity,
Granite	0.815
Dunite	0.856
Obsidian	0.862
Feldspar	0.870
Granite, rough	0.898
Silica sandstone, polished	0.909
Quartz sand, large grains	0.914
Dolomite, polished	0.929
Basalt, rough	0.934
Dolomite, rough	0.958
Asphalt paving	0.959
Concrete walkway	0.966
Water, with a thin film of petroleum	0.972
Water, pure	0.993

TABLE 5.2

Thermal properties of geologic materials and water at 20 °C

Geological materials	K Thermal conductivity	D Density	C Thermal capacity	P Thermal inertia
1. Basalt	0.0050	2.8	0.20	0.053
2. Clay soil (moist)	0.0030	1.7	0.35	0.042
3. Dolomite	0.0120	2.6	0.18	0.075
4. Gabbro	0.0060	3.0	0.17	0.055
5. Granite	0.0065	2.6	0.16	0.052
6. Gravel	0.0030	2.0	0.18	0.033
7. Limestone	0.0048	2.5	0.17	0.045
8. Marble	0.0055	2.7	0.21	0.056
9. Obsidian	0.0030	2.4	0.17	0.035
10. Peridotile	0.0110	3.2	0.20	0.084
11. Pumice loose	0.0006	1.0	0.16	0.009
12. Quartzite	0.0120	2.7	0.17	0.074
13. Rhyolite	0.0055	2.5	0.16	0.047
14. Sandy gravel	0.0060	2.1	0.20	0.050
15. Sandy soil	0.0014	1.8	0.24	0.024
16. Sandstone, quartz	0.00622	2.5	0.19	0.054
17. Serpentine	0.0072	2.4	0.23	0.063
18. Shale	0.0030	2.3	0.17	0.034
19. Slate	0.0050	2.8	0.17	0.049
20. Syenite	0.0044	2.2	0.23	0.047
21. Tuff, welded	0.0028	1.8	0.20	0.032
22. Water	0.0013	1.0	1.01	0.0337

TABLE 5.3

Microwave dielectric Properties of Sample Materials

(Most at 3×10^9 Hz)

Material	$\varepsilon'/\varepsilon_0$	$\varepsilon''/\varepsilon_0$
Sandy, dry soil	2.55	0.006
Loamy, dry soil	2.44	0.001
Freshly fallen snow	1.20	0.0003
Distilled water	77	0.157
Mahogany	1.9	0.025

TABLE 6.1

Multispectral Scanner Characteristics

Spectral bands	0.5-0.6 um
	0.6-0.7 um
	0.7-0.8 um
	0.8-1.1 um
Swath width	185 km
Ground resolution	82 m
Bit rate	15 Mbits/sec
Quantization level	64 (6 bits)

TABLE 6.2

Thematic Mapper Characteristics

Spectral Band (um)	Radiometric Sensitivity (NEΔP%)	Application
0.45-0.52	0.8	Soil type discrimination, soil/vegetation difference, coastal water mapping
0.52-0.6	0.5	Vegetation vigor and growth rate
0.63-0.69	0.5	Chlorophyll absorption/species differentiation, crop classification, ice and snow mapping
0.76-0.9	0.5	Water body delineation, biomass survey
1.55-1.75	1.0	Snow/cloud differentiation, vegetation moisture conditions
2.08-2.35	2.4	Distinguish hydrothermally altered zones from nonaltered zones
10.4-12.5		Surface temperature measurement land use, plant heat stress
Swath width	185 km	
Ground resolution	30 m on first 6 channels (bands 1-5, 7) 120 m on thermal IR channel (band 6)	
Data are	85 Mbits/sec	
Quantization level	256 (8 bits)	

Table 6.3

Characteristics of IRS IA LISS I and II

Sensors	Swath	Resolution
LISS I one Camera	148.48 km	72.5 km
LISS II Two Camera	145.48 km	36.25 m

Wavelength ranges of LISS I and II and its application

Band	Spectral range	Application
1	0.45 - 0.52 mm	Sensitivity to sedimentation deciduous/conferous forest cover discrimination
2	0.52 - 0.59	Green reflectance of healthy vegetation
3	0.62 - 0.68	Sensitivity to chlorophyll absorption by vegetation differentiation of soil and geological boundaries
4	0.77 - 0.86	Sensitive to green bio mass and moisture in vegetation

Table 6.4

Characteristics of SPOT.

Sensors	Wavelength band mm	Resolution
High Resolution visible (HRV)		
Multispectral mode		
Band 1	0.50 - 0.59	20 m
Band 2	0.61 - 0.68	20 m
Band 3	0.79 - 0.89	20 m
Panchromatic mode	0.51 - 0.73	10 m
Image format : 60 km swath width (nadir).		

Table 6.5

Characteristics of HCMR

Sensors	Wavelength (mm)	Resolution	Swath	Range
HCMR Heat Capacity Mapping Radiometer				
Visible Channel	0.5 - 1.1	500 m	716 km	0-100% Albedo
Thermal Channel	10.5 - 12.5	600 m	716 km	260-340 kelvin

TABLE 6.6

SMMR Instrument Characteristics (Norminal)

Characteristics	1	2	3	4	5
Frequency (GHz)	6.6	10.69	18	21	37
RF bandwidth (MHz)	220	220	220	220	220
Integration time (msec)	126	62	62	62	30
Sensitivity, T_{rms} (K)	0.9	0.9	1.2	1.5	1.5
Dynamic range (K)	10-330	10-330	10-330	10-330	10-330
Absolute accuracy (K) (long-term)	2	2	2	2	2
IF frequency range (MHz)	10-110	10-110	10-110	10-110	10-110
Antenna beamwidth (deg)	4.2	2.6	1.6	1.4	0.8
Antenna beam efficiency (%)	87	87	87	87	87

TABLE 7.1

Orbital Parameters of Certain Satellites

Sr. No.	Satellite name	Orbit type & altitude	Period and equator and crossing time (Local)	Repeat cycle (days)
1.	LANDSAT 1,2,3	Sun-synchronous 919 km.	--- 9.30 hrs	18
2.	NOAA 6,7,8,9 (TIROS N series)	Sun-synchronous 833-870 km.	101.6-102.4 mts 7.30, 19.30, 14.00, 02.00 hrs	1/2
3.	LANDSAT 4,5	Sun-synchronous 705 km.	99 mts 9.45 hrs.	16
4.	NIMBUS - 7	Sun-synchronous 995 km.	104 mts	16
5.	Heat capacity Mapping mission (HCMM)	Sun-synchronous 620 km.	---	16
6.	SPOT	Sun-synchronous 832 km	10.30 hrs	26
7.	IRS - 1	Sun-synchronous 900 km.	103.2 mts	22
8.	METEOSAT 1,2	Geostationary 35900 km.	24 hrs	---
9.	APPLE	Geostationary 36000 km.	24 hrs	---
10.	INSAT 1B	Geostationary 36000 km.	24 hrs	---
11.	INSAT 1C	Geostationary 36000 km.	24 hrs	---
12.	Seasat	800 km.	100.75 mts	152
13.	Bhaskara I & II	Inclined orbit 525 km	---	---

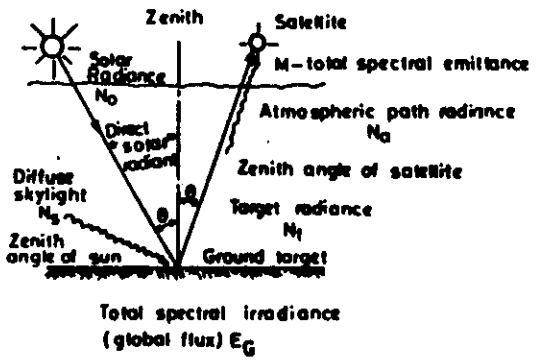

FIG.1.1a. Concepts of visible & near IR remote sensing

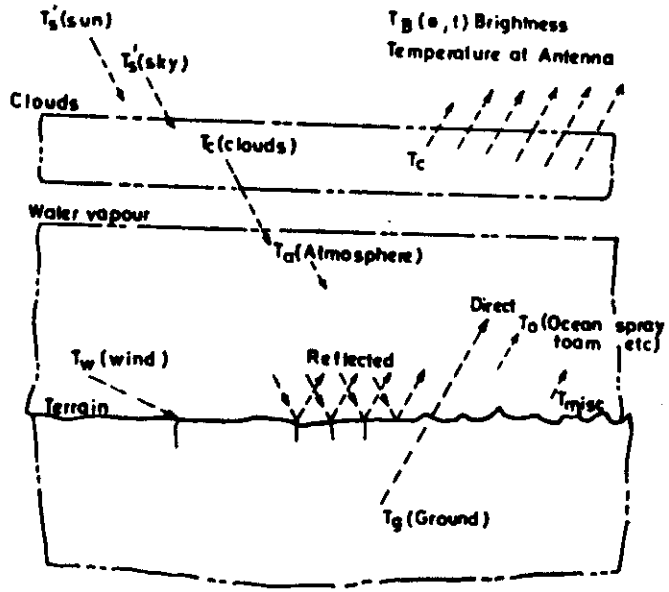

FIG. 1.1b Concepts of remote sensing in thermal and microwave regions of EMR

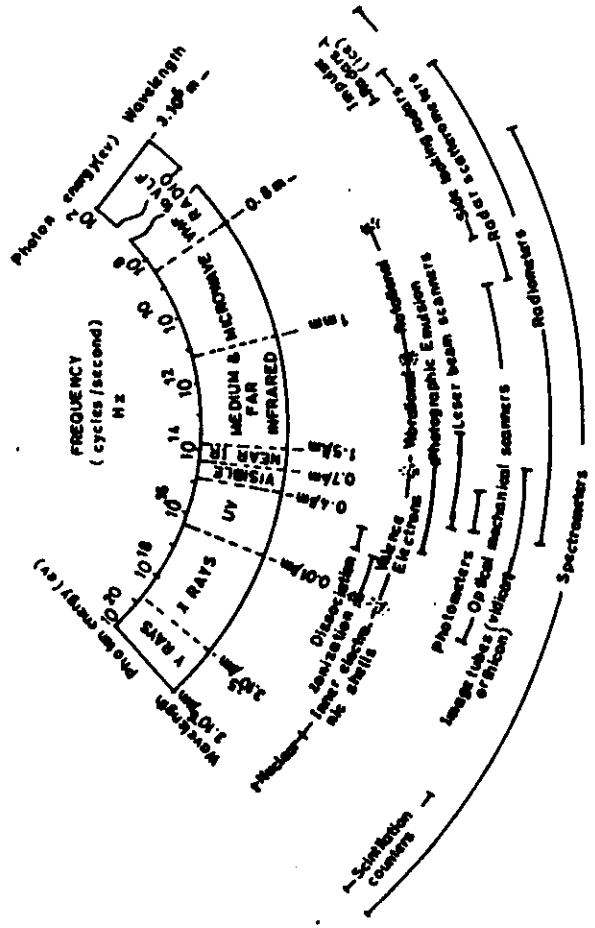

FIG. 2.1 The electromagnetic spectrum

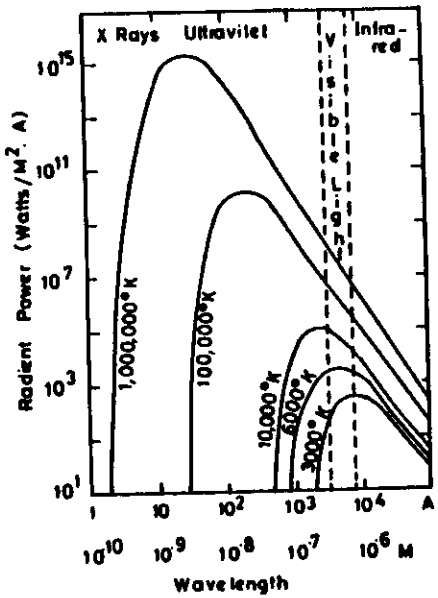

FIG. 3.1 Energy Distribution from a black body at various temperatures derived from the Planck equation

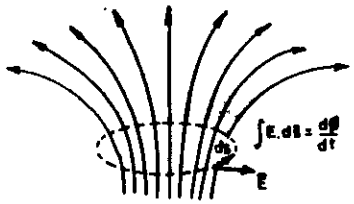

FIG 3.2 An illustration of Faradays induced emf law

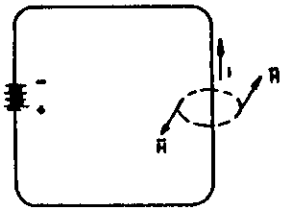

FIG 3.3 An illustration of Ampere's circuital law

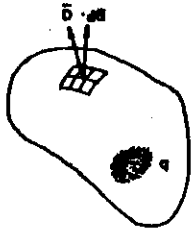

FIG 3.4 An illustration of Gauss's law

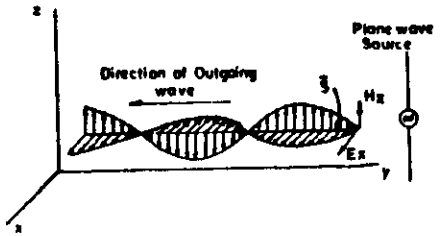

FIG. 3.5 Electromagnetic wave representation

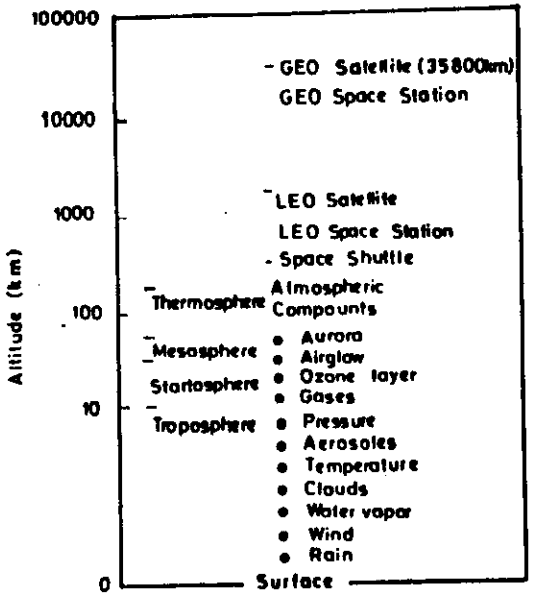

FIG. 4.1 Structure of atmosphere

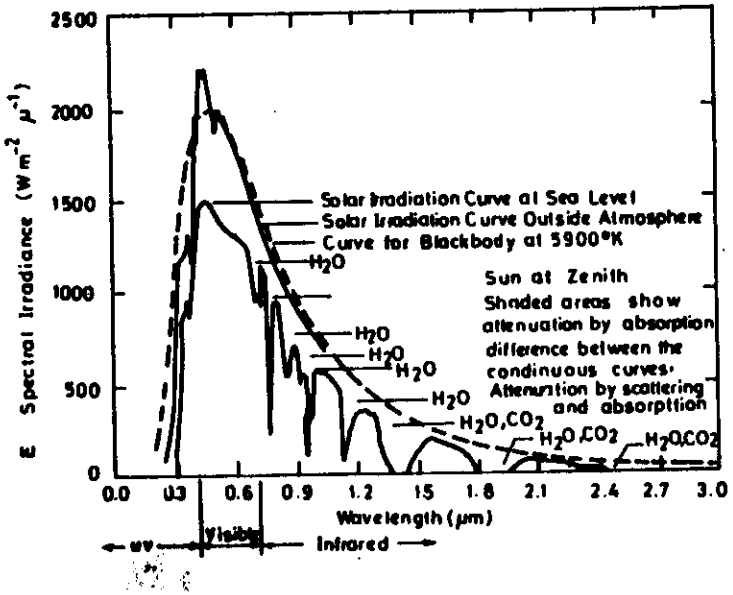

FIG. 4.2 Sun illumination spectral irradiance at the earth's surface

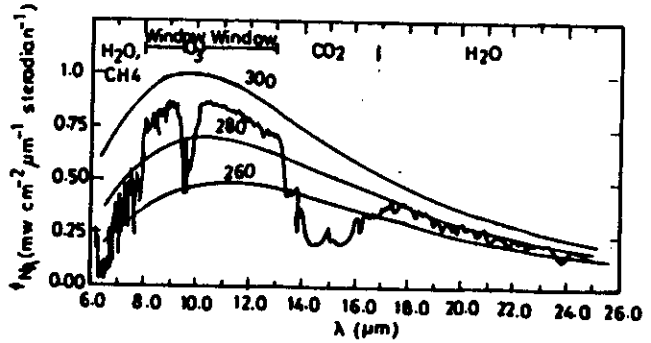

FIG. 4.3 Nadir radiance measured from a satellite (curve with structure) The smooth curves give values of blackbody radiances at the indicated temperature in degrees Kelvin

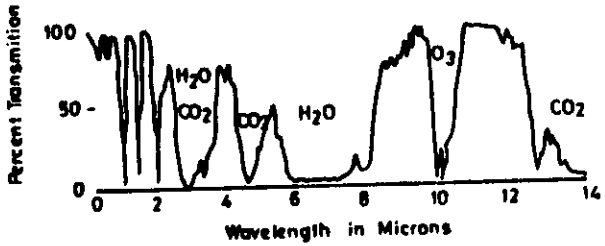

FIG 4.4 Atmospheric absorption schematic for the ultraviolet, visible, infrared, and the portion of the thermal infrared recorded by remote sensors (3.5μm-14 μm)

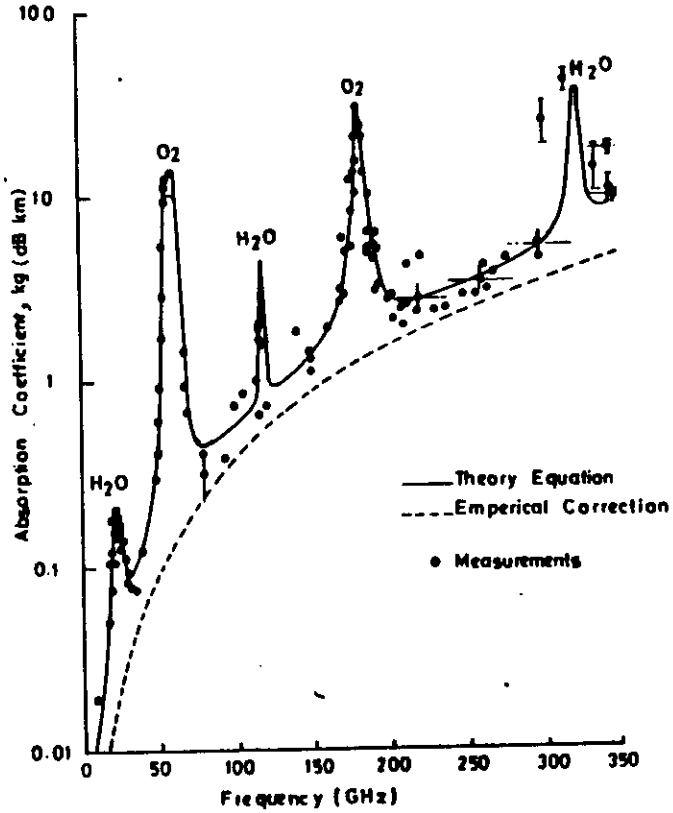

FIG 4.5 Microwave absorption due to atmospheric gases

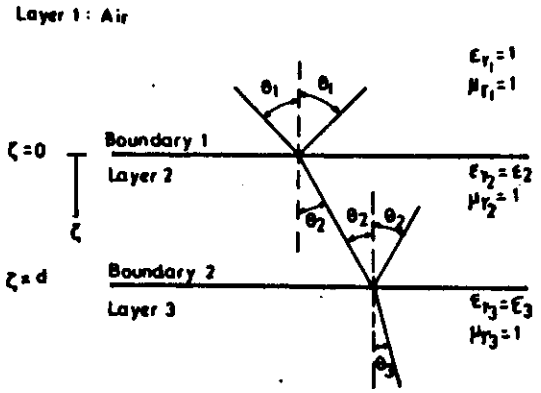

FIG. 5.1 Interaction process of EM radiation with layered media

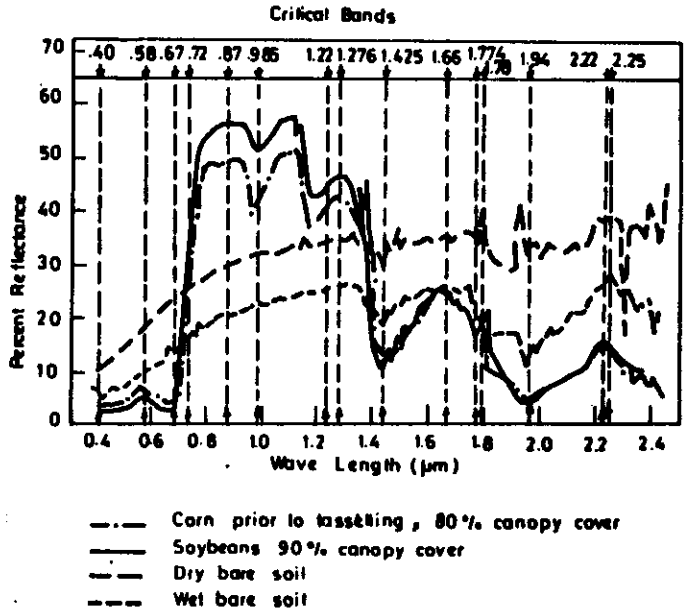

FIG. 5.2 Spectral reflectance of a variety of biological materials Reflectence of some cultivated vegetation compared to reflectence of bare soil and wet soil

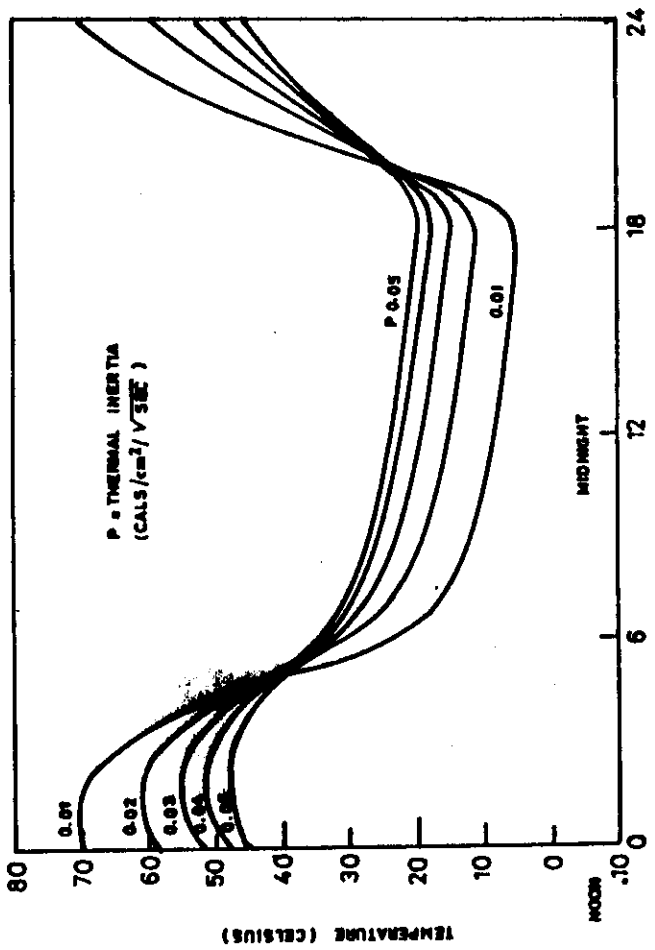

FIG.5.3 : Diurnal surface temperature variations computed for materials with different thermal inertias. (Reproduced from Farrow, 1975)

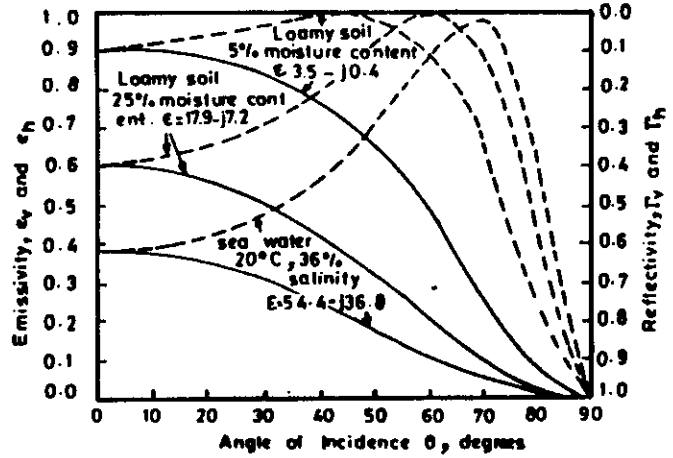

FIG. 5.4 Calculated reflectivities and emissivities as a function of incidence angle at 10 GHz. Calculation based on plane-surface model

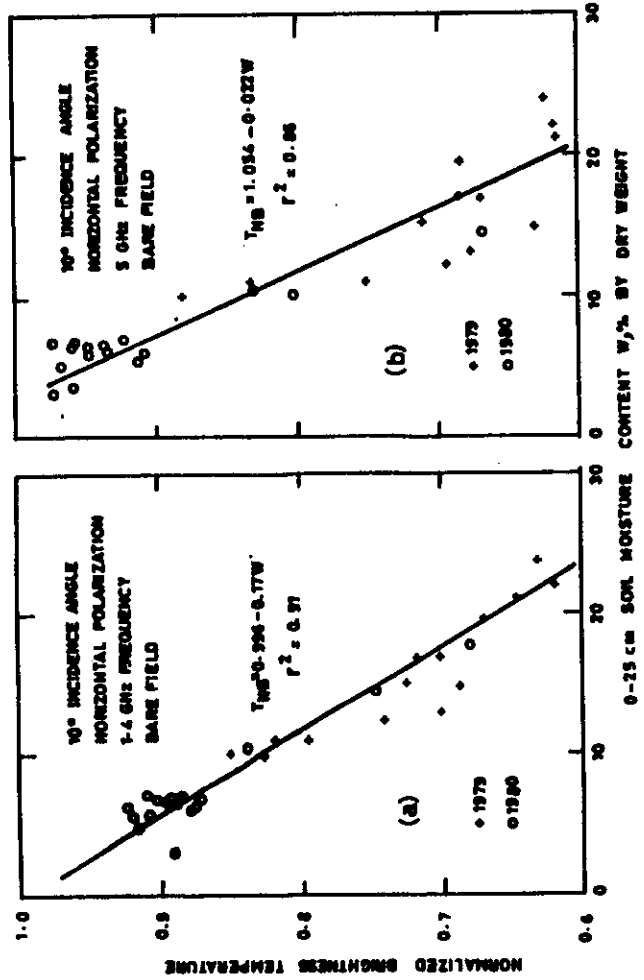

FIG. 5.5: The variation of normalized brightness temperatures with soil moisture content in the top 2.5 cm. layer: (a) 1.4 GHz frequency and (b) 5 GHz frequency. The measurements were made over bare fields in both 1979 and 1980 at 10° incidence angle and horizontal polarization.

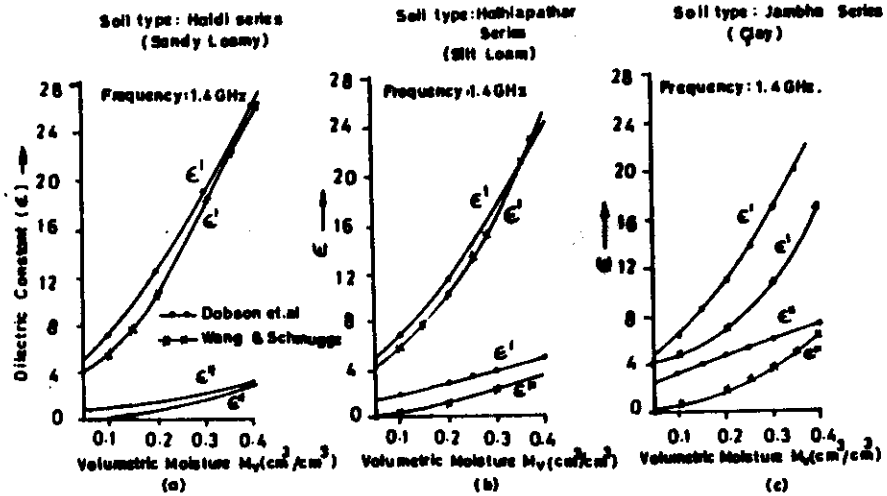

FIG 5.6 Soil moisture dependence of dielectric constant (ε) at 1.4 GHz calculated by semiempirical models for (a) Haldi series (sandy loam) (b) Hathlapathar series (silt loam) (c) Jambha series (clay)

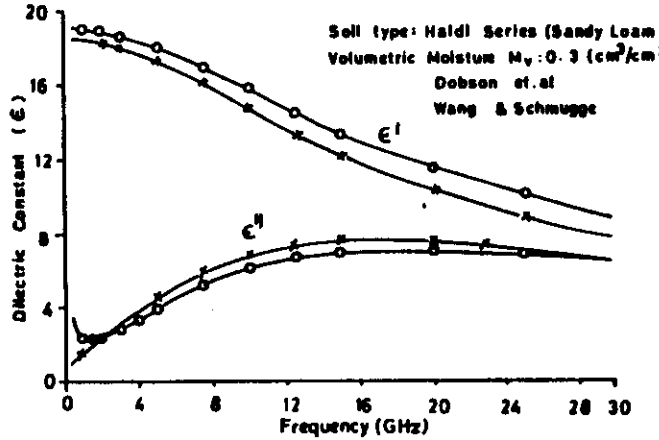

FIG. 5.7 Frequency dependence of the semiempirical models at moisture content (M = 0.3) for Haldi series

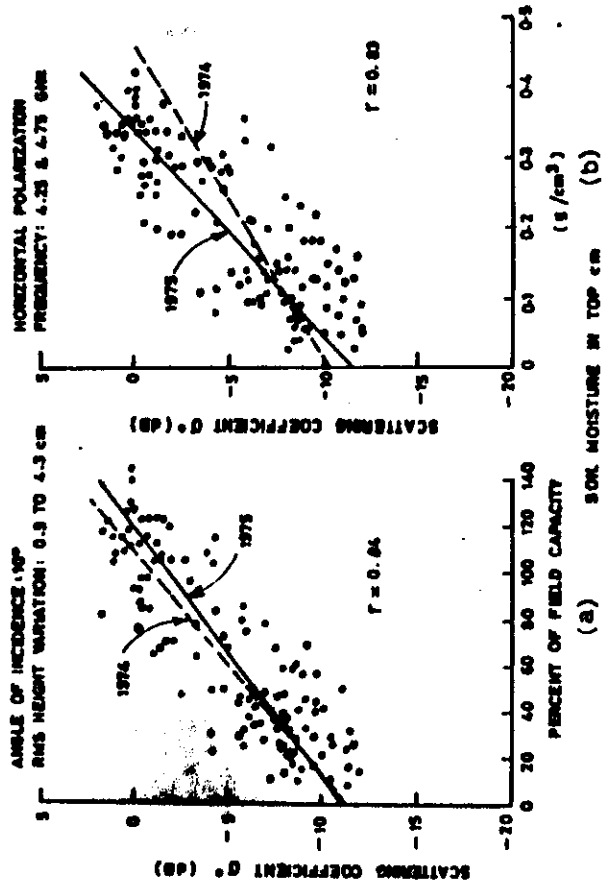

FIG.5.8: Backscattering coefficient plotted as function of soil moisture given (a) in percent of field capacity of the top 1cm and (b) volumetrically in the top 1cm. Data from bare soil experiments in 1974 (•) and 1975 (•) are combined (Batlivala and Ulaby, 1977, Ulaby et al., 1978)

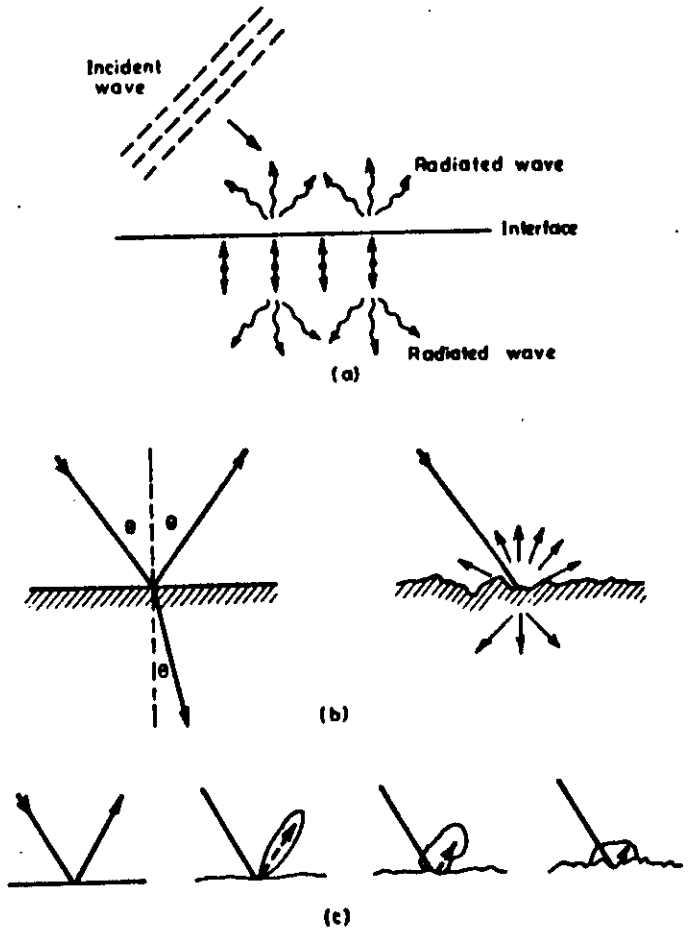

FIG. 5.9 a) An incident wave on a dielectric half-space will excite the dielectric atoms, which become small oscillating dipoles. These dipoles reradiate waves in both half spaces b) In the case of a flat interface (left), the reradiated waves are in two specific directions; reflection and refraction. In the case of a rough surface (right) waves are reradiated in all directions. c) Pattern of reradiated waves in the upper half-space for increasingly rough interfaces.

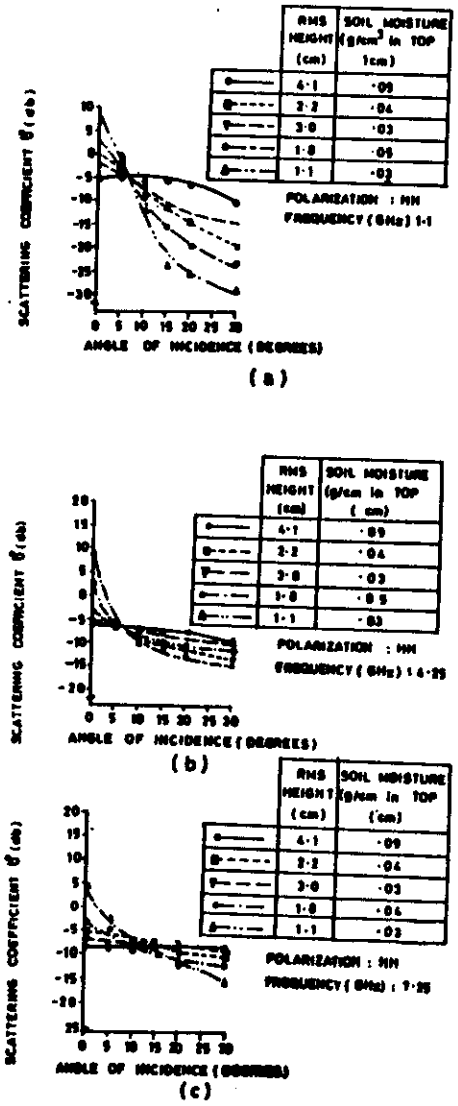

Fig 5.10 Angular response of scattering for the five fields for low levels of moisture content at (a) 1·1GHz, (b) 4·25GHz and (c) 7·25GHz

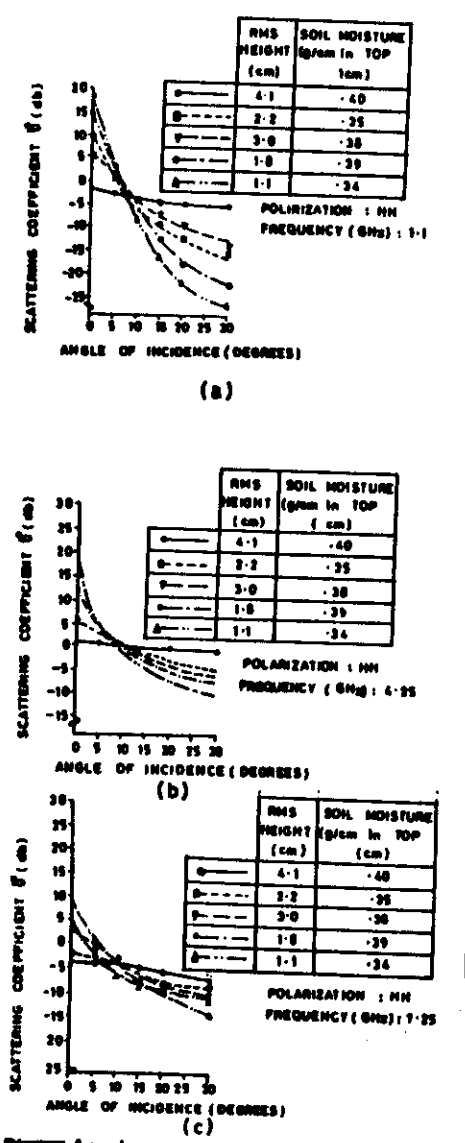

Fig 5.10 Angular response of scattering coefficient for the five fields for high levels of moisture content at (a) 1·1GHz (b) 4·25GHz and (c) 7·25 GHz

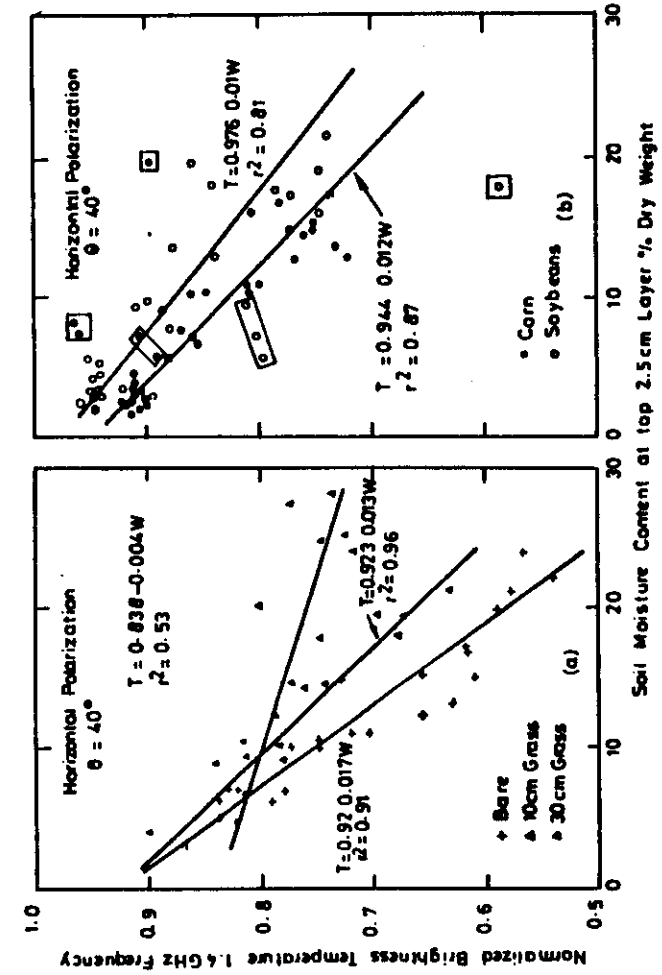

FIG. 5.11 a The normalized brightness temperatures at incidence angle of 40° plotted as a function of soil moisture content in the top 2.5 cm layer for bare and vegetated fields: (a) bare, 10 cm grass and 30 cm grass fields and (b) soybean and corn fields. The measurements were made at 1.4 GHz and horizontal polarization

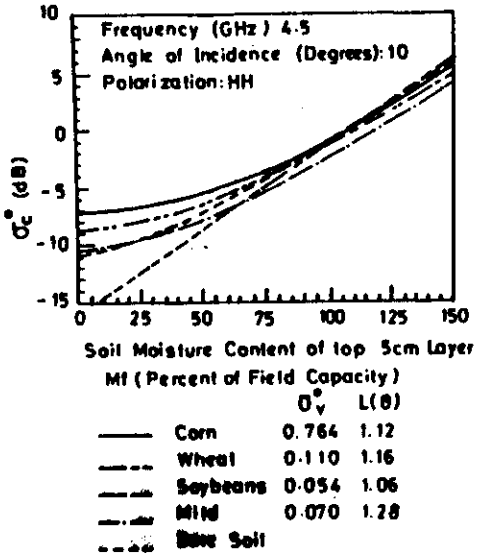

FIG. 5.11 b Variation of canopy backscattering coefficient with soil moisture content for individual crop types

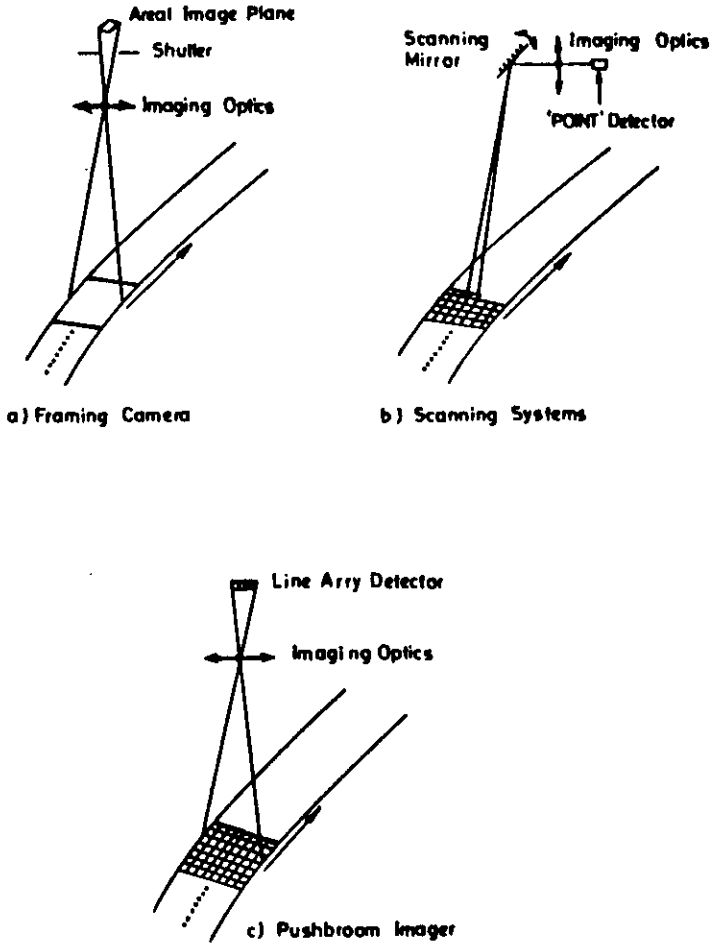

FIG. 6.1 Different types of imaging system

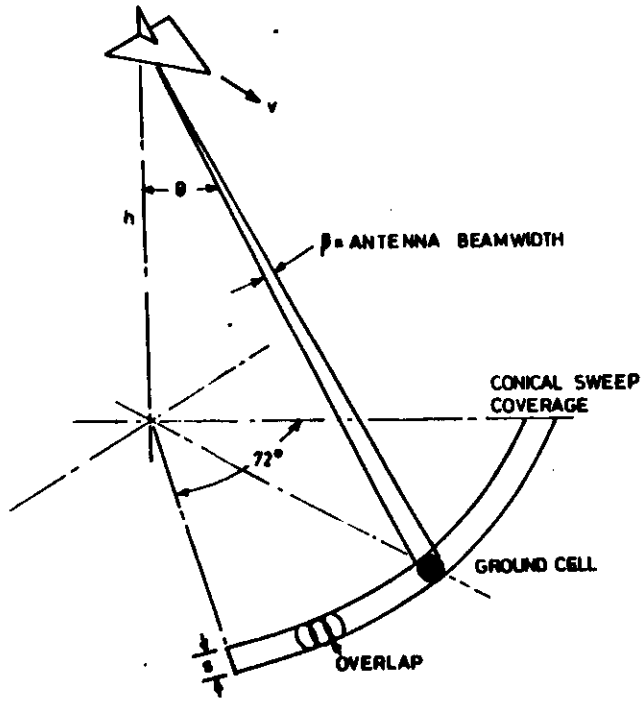

FIG. 6.2 Geometry for airborne conically scanned imaging radiometer

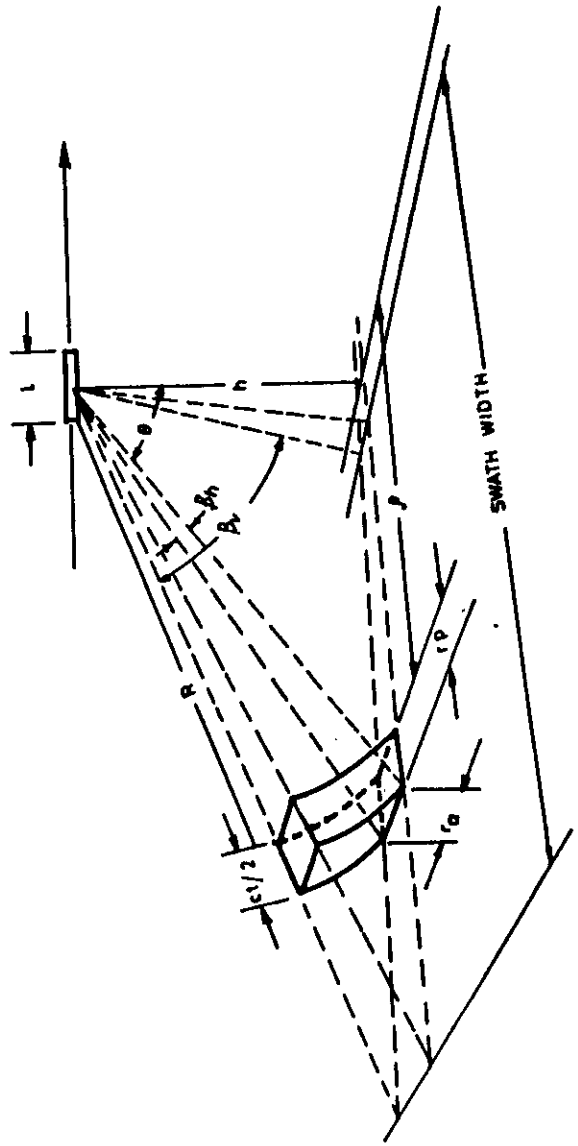

FIG. 6.3 SLAR Geometry

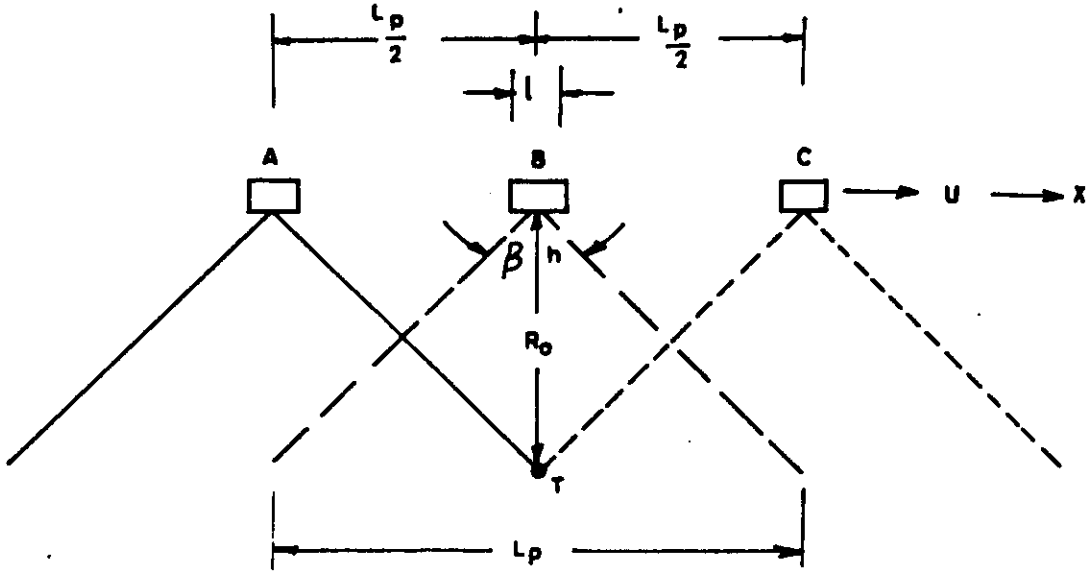

(a) Antena beams Illuminating Target at T

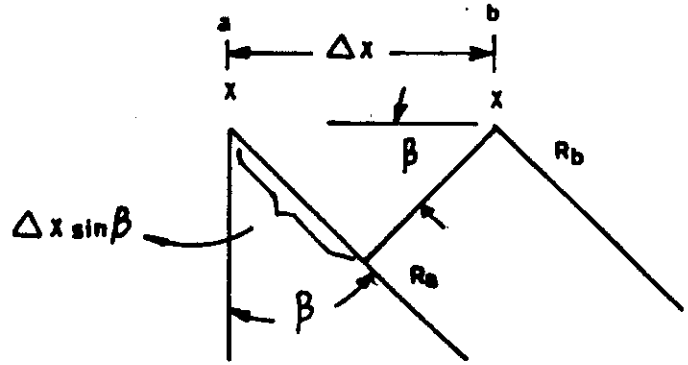

(b) Two Adjacent Elements in Synthetic Arry

FIG. 6.4 An Illustration of synthetic aperature approach